

Neon NTT: Faster Dilithium, Kyber, and Saber on Cortex-A72 and Apple M1

Hanno Becker¹, Vincent Hwang^{2,3}, Matthias J. Kannwischer³, Bo-Yin Yang³
and Shang-Yi Yang⁴

¹ Arm Research, Cambridge, UK

hanno.becker@arm.com

² National Taiwan University, Taipei, Taiwan

vincentvbh7@gmail.com

³ Academia Sinica, Taipei, Taiwan

matthias@kannwischer.eu, by@crypto.tw

⁴ Chelpis Co. Ltd., Taipei, Taiwan

nick.yang@chelpis.com

Abstract. We present new speed records on the Armv8-A architecture for the lattice-based schemes Dilithium, Kyber, and Saber. The core novelty in this paper is the combination of Montgomery multiplication and Barrett reduction resulting in “Barrett multiplication” which allows particularly efficient modular one-known-factor multiplication using the Armv8-A Neon vector instructions. These novel techniques combined with fast two-unknown-factor Montgomery multiplication, Barrett reduction sequences, and interleaved multi-stage butterflies result in significantly faster code. We also introduce “asymmetric multiplication” which is an improved technique for caching the results of the incomplete NTT, used e.g. for matrix-to-vector polynomial multiplication. Our implementations target the Arm Cortex-A72 CPU, on which our speed is $1.7\times$ that of the state-of-the-art matrix-to-vector polynomial multiplication in `kyber768` [Nguyen–Gaj 2021]. For Saber, NTTs are far superior to Toom–Cook multiplication on the Armv8-A architecture, outrunning the matrix-to-vector polynomial multiplication by $2.0\times$. On the Apple M1, our matrix-vector products run $2.1\times$ and $1.9\times$ faster for Kyber and Saber respectively.

Keywords: NIST PQC · Armv8-A · Neon · Dilithium · Kyber · Saber

1 Introduction

When large quantum computers arrive, Shor’s algorithm [Sho97] will break almost all currently deployed public-key cryptography by solving the integer factorization and the discrete logarithms problems. Preparing for this, the U.S. National Institute of Standards and Technology (NIST) has initiated a process to select new cryptosystems that withstand the increased capabilities of quantum computers – an area known as Post-Quantum Cryptography (PQC). This process naturally divides into categories of digital signatures and key encapsulation mechanisms (KEMs) [NIS] and is currently in the third round, where 7 finalists and 8 alternate candidates still compete [AASA⁺20].

Undoubtedly, the scheme(s) selected at the end of the NIST PQC competition will become prominent computational workloads of the future. It is therefore important to understand their performance and resource characteristics on the hugely diverse spectrum of today’s and upcoming computing platforms, ranging from low-power IoT devices over desktops to high-end data center cores, to name some. Representative of the former, the focus of performance analysis of PQC on embedded devices has so far been the Arm[®]

Cortex[®]-M4 CPU. Representative of the latter, the focus of performance analysis on high-end cores has so far been the AVX2-capable Intel[®] CPUs Haswell and Skylake.

In this article, we contribute to the performance analysis of prominent PQC candidates on CPUs implementing the application profile / A-profile of the Arm architecture¹ – an area which, despite its importance, has been comparatively little studied so far. CPUs implementing the A-profile are ubiquitous, and form a wide spectrum in themselves: It contains power-efficient CPUs like the Cortex-A7 processor for Linux-capable embedded IoT devices, cores for the mobile and desktop market like the Cortex-A78 processor, as well as the Arm[®] Neoverse[™] IP for infrastructure applications, for example, the Arm Neoverse-based AWS Graviton processors. The Fugaku supercomputer ranked as the fastest supercomputer in the world in 2020 and 2021 [TOP20, TOP21], is also based on a core implementing the A-profile. Considering the breadth of use and availability of A-profile cores in the computing ecosystem, it is therefore important to include them in the performance evaluation for PQC.

Another axis of distinction within the A-profile is the specific version of the architecture, such as Armv7-A, Armv8-A, and, as of late, Armv9-A, and their respective sets of extensions. In this article, we focus on implementations of PQC on CPUs based on the 64-bit Armv8-A architecture, leveraging the availability of the Armv8-A version of the Arm[®] Neon[™] Single Instruction Multiple Data (SIMD) instruction set. We do not study implementations based on the Neon instruction set for Armv7-A or implementations based on the Scalable Vector Instructions SVE and SVE2 here – this is left for future work.

Returning to the nature of the PQC workloads themselves: Many of the remaining NISTPQC candidate schemes are based on so-called structured lattices, for which the central arithmetic operation is modular polynomial multiplication. A central implementation technique for such polynomial multiplication is the Number-Theoretic Transform (NTT), an integer-analog of the Fast Fourier Transform.

In this work, we explore the use of NTTs in implementing the NISTPQC structured lattice finalist candidates. It has always been a point of interest to determine the realms of applicability for various advanced multiplication techniques, and in addition to finding out how well NTTs do, we also compare them to other approaches towards polynomial multiplication, in particular Toom-Cook/Karatsuba.

Contributions. We exhibit NTT-based implementations of NISTPQC cyclotomic-ring lattice candidates for CPUs implementing the A-profile of the Arm architecture, leveraging the Neon vector extension. We optimized mainly for the common Cortex-A72 CPU (used e.g. in the Raspberry Pi 4), and somewhat for the Apple M1, a high-end desktop core.

We improve on old and discover new implementation techniques, including a Barrett-reduction based one-known-factor multiplication, which we show to be roughly equivalent to the Montgomery multiplication technique of [Sei18], but particularly suitable for Neon.

We also introduce the trick of “asymmetric base multiplication” which is applicable whenever we are caching incomplete NTT results (i.e., Kyber/Saber). Furthermore, we improve on the best-known two-unknown-factors multiplications and Barrett reduction sequences in the literature.

Code. Our code is available at <https://github.com/neon-ntt/neon-ntt>.

Related Work. The most recent work on lattice-based cryptography on the Armv8-A architecture using the Neon vector extension is by Nguyen and Gaj [NG21] and Sanal et al. [SKS⁺21]. NTT is frequently used in the context of polynomial multiplications

¹The Arm architecture has three profiles – application (A), real-time (R) and embedded (M) – and each Arm-based CPU implements a version of one of those profiles. The well-studied Cortex-M4 processor, for example, belongs to the M-profile.

Table 1: Kyber and Saber Parameter Sets

name	l	(d_1, d_2)	$\eta(s s')$	$\eta(e e' e'')$	name	l	$T = 2^{\epsilon_T}$	η
Kyber512	2	(10, 4)	6	4	LightSaber	2	2^3	10
Kyber768	3	(10, 4)	4	4	Saber	3	2^4	8
Kyber1024	4	(11, 5)	4	4	FireSaber	4	2^6	6

which form the basis of almost all lattice-based PQC. Recently, NISTPQC third-round candidates have been implemented for the Arm Cortex-M3 and Cortex-M4 using NTTs. The most relevant works are Botros et al. [BKS19] and Alkim et al. [ABCG20] on Kyber, Greconici et al. [GKS21] on Dilithium, Chung et al. [CHK⁺21] on Saber and NTRU, and Alkim et al. [ACC⁺21] on NTRU Prime.

Addendum: Related work. One of our contributions, the “Barrett multiplication” algorithm, is very close to *Shoup’s modular multiplication* algorithm [Har14, Algorithm 3], a fact which we got aware of only after finalizing the camera-ready version of this paper. Like Barrett multiplication, Shoup’s multiplication computes a one-known-factor modular multiplication with essentially three integer multiplications, at the expense of a precomputation on the known factor. Our work furthers the understanding and concrete implementation of this efficient technique by (a) applying it in the signed context, (b) establishing a relation with Montgomery multiplication which we believe has not been noted before, and (c) by allowing an arbitrary integer approximation which is essential in making the algorithm amenable for implementation through common fixed-point instructions. We appreciate any clarification about other prior art that we might have missed.

Structure of the paper. This paper is structured as follows: Section 2 introduces the schemes we implement, the Armv8-A microarchitecture, and the mathematical background on NTTs. In Section 3, we present more mathematics in the form of reductions for the implementations used in this paper. In Section 4, we go through the implementation details of the different schemes. In Section 5, we show performance numbers and conclude.

2 Preliminaries

2.1 Kyber

Kyber [ABD⁺20b] is a NISTPQC finalist candidate lattice-based key encapsulation mechanism based on the Module Learning With Errors (M-LWE) problem. The module is of dimension $\ell \times \ell$ over the ring $R_q = \mathbb{F}_q[x]/\langle x^n + 1 \rangle$, with $q = 3329$ and $n = 256$. The Kyber KEM is derived *a la* [HHK17] from a CPA-secure Public-Key Encryption (PKE).

Please refer to algorithmic descriptions of the PKE in in Appendix A. In the CPA-secure key generation and encryption the rate-determining operations are $(\ell \times \ell) \times (\ell \times 1)$ matrix-to-vector polynomial multiplications $A^T \cdot s$ and As' (`MatrixVectorMul`). In decryption, it is the $\ell \times 1$ inner product of polynomials $b'^T \cdot s$ (`InnerProd`). Note that [ABD⁺20b] specifies that *we do all multiplications via incomplete NTT, and NTT results are in bit-reversed order*. The public matrix A is sampled in (incomplete) NTT domain by expanding a seed using the extendable-output function (XOF) SHAKE128. There is 1 matrix-to-vector polynomial multiplication and 0, 1, and 2 inner products of polynomials in each of key generation, encapsulation, and decapsulation respectively.

Parameters. The module dimension ℓ , the rounding parameters (d_1, d_2) , and the width of the centered binomial distribution η vary according to the parameter sets `Kyber-512`, `-768`, and `-1024` (targeting the NIST security levels 1, 3, and 5 respectively, cf. Table 1).

2.2 Saber

Saber [DKRV20] is a NISTPQC finalist candidate lattice-based key encapsulation mechanism based on the Module Learning With Rounding (M-LWR) problem. The module is of dimension $\ell \times \ell$ over the ring $R_q = \mathbb{Z}_q[x]/\langle x^n + 1 \rangle$, with $q = 2^{13}$ and $n = 256$. Similar to Kyber, the Saber KEM is built on top of a CPA-secure PKE via the CCA-transform *ala* [HHK17]. For algorithmic descriptions of the Saber PKE see Appendix B.

In CPA-secure key generation and encryption, the rate-determining operations are $(\ell \times \ell) \times (\ell \times 1)$ matrix-to-vector polynomial multiplications $A^T \cdot s$ and As' (`MatrixVectorMul`). In decryption, it is the $\ell \times 1$ inner product of polynomials $b^T \cdot s$ (`InnerProd`). There is 1 `MatrixVectorMul` in key generation; 1 `MatrixVectorMul` + 1 `InnerProd` in encapsulation; and 1 `MatrixVectorMul` + 2 `InnerProd` in decapsulation, as decapsulation needs a full re-encryption.

Note that Saber’s base ring $\mathbb{Z}_{2^{13}}$ is not a field and thus not directly amenable for application of the NTT. Accordingly, the specification samples the public matrix A in polynomial domain.

Parameters. The module dimension l , the rounding parameter T , and the secret distribution parameter η vary according to the parameter sets `Lightsaber`, `Saber`, and `Firesaber` (respectively targeting the NIST security levels 1, 3, and 5, cf. Table 1).

2.3 Dilithium

Dilithium [ABD+20a] is a NISTPQC [NIS] finalist digital signature scheme based on the M-SIS (Module Small Integer Solutions) and M-LWE problems. The module is of dimension $k \times \ell$ over the ring $R_q = \mathbb{F}_q[x]/\langle x^{256} + 1 \rangle$ with $q = 2^{23} - 2^{13} + 1 = 8380417$.

For algorithmic descriptions see Appendix C. The core operation of key generation, signature generation, and signature verification is the $(k \times \ell) \times (\ell \times 1)$ matrix-to-vector polynomial multiplications As_1 , Ay , and Az (resp.) (`MatrixVectorMul`). In signature generation, this operation is particularly time-consuming since it is executed in a loop. Similar to Kyber, Dilithium builds a (complete) NTT into the specification, i.e., A is sampled in NTT domain using the XOF SHAKE256.

Table 2: Dilithium parameter sets

Name	NIST level	(k, ℓ)	η	β	ω	$ pk $	$ sig $	exp. iterations
Dilithium2	2	(4, 4)	2	78	80	1312	2420	4.25
Dilithium3	3	(6, 5)	4	196	55	1952	3293	5.1
Dilithium4	5	(8, 7)	2	120	75	2592	4595	3.85

Parameters. Dilithium has parameter sets `Dilithium2`, `Dilithium3`, and `Dilithium5` targeting the corresponding NIST security levels. For all parameter sets $\gamma_1 = (q - 1)/16 = 523776$ and $\gamma_2 = \gamma_1/2 = 261888$. For each parameter set, the remaining parameters are given in Table 2. The parameters consist of the matrix dimension (k, ℓ) , the sampling bounds of the secret η , and the rejection thresholds β and ω .

2.4 Modular arithmetic

In this section, we establish some basic facts and notation about modular arithmetic which we will use throughout the paper.

Notation. We will denote $\llbracket \cdot \rrbracket$ any “integer approximation”, by which we mean $\llbracket \cdot \rrbracket : \mathbb{Q} \rightarrow \mathbb{Z}$ with $|z - \llbracket z \rrbracket| \leq 1$ for all $z \in \mathbb{Z}$. Examples include the rounding functions $\lfloor \cdot \rfloor$, $\lceil \cdot \rceil$, $\lfloor \cdot \rfloor$, but also e.g. the $2\mathbb{Z}$ -valued $\lfloor z \rfloor_2 := 2 \lfloor \frac{z}{2} \rfloor$, which will be of special interest later. Note that we do not require $\llbracket z \rrbracket = z$ for all $z \in \mathbb{Z}$, and it does in fact not hold for $\lfloor \cdot \rfloor_2$.

Let $N \in \mathbb{N}$, henceforth called the *modulus*; in our application we will have either $N = 2^k$ or $N = q$ an odd prime. We denote $\mathbb{Z}_N := \mathbb{Z}/N\mathbb{Z}$ (or \mathbb{F}_q if $N = q$ is a prime) the quotient ring of \mathbb{Z} by the equivalence relation $x \equiv_N y$, identifying two integers which leave the same residue after division by N . For $z \in \mathbb{Z}$, we denote $\underline{z} \in \mathbb{Z}_N$ its residue class; in the case of a 2-power N , we use the notation \bar{z} instead.

Both the signed interval $S_N := \{-\lfloor \frac{N}{2} \rfloor, -\lfloor \frac{N}{2} \rfloor + 1, \dots, \lfloor \frac{N-1}{2} \rfloor - 1, \lfloor \frac{N-1}{2} \rfloor\}$ and the unsigned interval $U_N := \{0, 1, \dots, N-1\}$ are fundamental domains for \equiv_N ; for $z \in \mathbb{Z}$, we denote $z \bmod^\pm N \in S_N$ and $z \bmod^+ N \in U_N$ the unique representatives of z in S_N and U_N and call them *canonical signed representative* and *canonical unsigned representative*, respectively. For example, $-15 \bmod^\pm 13 = -2$ and $-15 \bmod^+ 13 = 11$.

The canonical signed and unsigned representatives are related to the integer approximations $\lfloor \cdot \rfloor$ and $\lceil \cdot \rceil$ via $z \bmod^\pm N = z - N \lfloor \frac{z}{N} \rfloor$ and $z \bmod^+ N = z - N \lfloor \frac{z}{N} \rfloor$. More generally, we can define $z \bmod^{\llbracket \cdot \rrbracket} N := z - N \llbracket \frac{z}{N} \rrbracket$ for any integer approximation $\llbracket \cdot \rrbracket$.

Example 1. We consider $z \bmod^{\lfloor \cdot \rfloor_2} N$ associated with $\lfloor z \rfloor_2 = 2 \lfloor \frac{z}{2} \rfloor$. In this case, $z \bmod^{\lfloor \cdot \rfloor_2} N$ is a representative of z modulo N within $\{-N, \dots, N\}$ of the same parity as z . For example, if z is even, we have $z \bmod^{\lfloor \cdot \rfloor_2} N = z \bmod^\pm N$ if $z \bmod^\pm N$ is even, and $z \bmod^{\lfloor \cdot \rfloor_2} N = z \bmod^\pm N - \text{sign}(z \bmod^\pm N)N$ otherwise.

If $\llbracket \cdot \rrbracket$ satisfies $\llbracket z+1 \rrbracket = \llbracket z \rrbracket + 1$, then $z \bmod^{\llbracket \cdot \rrbracket} N$ descends to a function $\mathbb{Z}_N \rightarrow \mathbb{Z}$; this is the case for $\lfloor \cdot \rfloor$ and $\lfloor \cdot \rfloor_2$, and we will also use $\underline{z} \bmod^\pm N$ and $\underline{z} \bmod^+ N$ for $\underline{z} \in \mathbb{Z}_N$.

We will need the following fact:

Fact 1. Let $R = 2^n$ and $\bar{x} \in \mathbb{Z}_R$. Then the following holds:

1. If $x \neq \overline{2^{n-1}} \in \mathbb{Z}_R$, then $(-x) \bmod^\pm R = -(x \bmod^\pm R)$.
2. If $x = \overline{2^{n-1}} \in \mathbb{Z}_R$, then $(-x) \bmod^\pm R = -(x \bmod^\pm R) - R$.

Beyond those canonical representatives, we will also be interested in non-unique representatives from intervals $\{-N', -N'+1, \dots, N'-1, N'\}$, where N' is suitably bounded with respect to N . By “algorithms for arithmetic modulo N ” we mean algorithms which compute addition and multiplication in \mathbb{Z}_N in terms of “small” representatives within those sets. The primary objective in designing such algorithms is the avoidance of generic integer division; a secondary goal is to avoid unnecessary reductions. Our main techniques are Montgomery and Barrett reduction, which we recall briefly now.

2.4.1 Barrett reduction

We have $z \bmod^\pm N = z - N \cdot \lfloor \frac{z}{N} \rfloor$. The idea behind Barrett reduction [Bar86] is to approximate $\frac{z}{N} = z \frac{R}{N} / R \approx z \lfloor \frac{R}{N} \rfloor / R$, so $z \bmod^\pm N \approx z - N \cdot \lfloor z \lfloor \frac{R}{N} \rfloor / R \rfloor$, where $\lfloor - \rfloor$ is a choice of integer approximation and $R = 2^n > N$ is fixed. Since $\lfloor \frac{R}{N} \rfloor$ can be precomputed, this provides an approximation to $z \bmod^\pm N$ relying solely on division by $R = 2^n$, which common hardware can realize as a bitshift. We denote the resulting approximation to $z \bmod^\pm N$ by $\mathbf{bar}_N^{\llbracket \cdot \rrbracket}(z)$, or $\mathbf{bar}_N^\pm(z)$ if $\llbracket \cdot \rrbracket = \lfloor \cdot \rfloor$. See Algorithm 1.

Algorithm 1 Barrett reduction	Algorithm 2 Montgomery reduction
Require: N modulus, $R = 2^n > N$	Require: N odd, $R = 2^n > N$
Require: $\lfloor \frac{R}{N} \rfloor \in \mathbb{Z}$ approx. of $\frac{R}{N}$.	Require: $T \in \mathbb{Z}$, $T \equiv \pm N^{-1} \pmod{R}$
Require: $z \in \mathbb{Z}$, $ z \leq R$, to be reduced	Require: $z \in \mathbb{Z}$, to be reduced
Ensure: $z' \equiv z \pmod{N}$, $ z' < \frac{3}{2}N$.	Ensure: $z' \equiv zR^{-1} \pmod{N}$, $ z' \leq \frac{ z }{2^n} + \frac{N}{2}$.
1: $t \leftarrow \lfloor z \lfloor \frac{R}{N} \rfloor / R \rfloor$	1: $k \leftarrow zT \bmod^{\pm} R$
2: $c \leftarrow \overline{N}t$	2: $c \leftarrow kN$
3: $\mathbf{bar}_N^{\lfloor \cdot \rfloor}(z) := z' \leftarrow z - c$	3: $\mathbf{mont}_N^{\pm}(z) := z' \leftarrow \frac{z \mp c}{R}$

Fact 2. For any choice of integer approximation $\lfloor \cdot \rfloor$, we have

$$|z \bmod^{\pm} N - \mathbf{bar}_N^{\lfloor \cdot \rfloor}(z)| \leq N \left\lceil \frac{|z|}{R} \right\rceil.$$

In particular, if $|z| \leq R$, we have $|\mathbf{bar}_N^{\lfloor \cdot \rfloor}(z)| < \frac{3}{2}N$.

Proof. The left hand side is equal to $N \left| \lfloor \frac{z}{N} \rfloor - \lfloor z \lfloor \frac{R}{N} \rfloor / R \rfloor \right| = N \left| \lfloor z \frac{R}{N} / R \rfloor - \lfloor z \lfloor \frac{R}{N} \rfloor / R \rfloor \right|$. Now, apply $|\lfloor a \rfloor - \lfloor b \rfloor| \leq \lceil a - b \rceil$ and the defining property $|\frac{R}{N} - \lfloor \frac{R}{N} \rfloor| \leq 1$. \square

Implementation considerations. In the context of Algorithm 1, the result has absolute value $|c - t| < \frac{3}{2}N$. If $N < \frac{R}{3}$, $c - t$ is a signed canonical representative modulo $R = 2^n$, and thus uniquely determined by its residue modulo 2^n . This observation allows us to perform steps 2 and 3 in Algorithm 1 in single-width arithmetic, leading to the presentation of Barrett reduction in terms of single-width operations alone (Algorithm 3).

Algorithm 3 Barrett reduction, implementation-view

Require: N modulus, $R = 2^n$ s.t. $N < \frac{R}{3}$.	
Require: $\lfloor \frac{R}{N} \rfloor \in \mathbb{Z}$ precomputed integer approximation of $\frac{R}{N}$.	
Require: $z \in \mathbb{Z}$ representative mod N with $ z \leq R$, to be reduced	
Ensure: $\mathbf{bar}_N^{\lfloor \cdot \rfloor}(z)$ representative of z with $ \mathbf{bar}_N^{\lfloor \cdot \rfloor}(z) < \frac{3}{2}N < \frac{R}{2}$.	
1: $t \leftarrow \lfloor z \lfloor \frac{R}{N} \rfloor / R \rfloor$	▷ Signed multiply-high with rounding
2: $\bar{c} \leftarrow \overline{N} \cdot t$	▷ Unsigned single-width multiply
3: $\bar{z} \leftarrow \bar{z} - \bar{c}$	▷ Unsigned single-width subtract
4: $\mathbf{bar}_N^{\lfloor \cdot \rfloor}(z) \leftarrow \bar{z} \bmod^{\pm} R$	▷ Canonical signed representative

2.4.2 Montgomery reduction

Like Barrett reduction, Montgomery reduction [Mon85] provides a way to trade expensive division by N for cheap division by a power of two.

The idea is simple: Assume we would like to reduce $z \in \mathbb{Z}$ with respect to the odd modulus N , and that z happens to be a multiple of $R = 2^n \in \mathbb{Z}$. Then the (cheaply computed) integer division $\frac{z}{R}$ is a representative of $\underline{z} \cdot \underline{R}^{-1} \in \mathbb{Z}_N$ which is shorter than z by n bits. In other words, if we accept “twisting” our target residue \underline{z} by some factor $\underline{R}^{-1} \in \mathbb{Z}_N$, we can shorten its representative.²

If the given representative $z \in \mathbb{Z}$ is not evenly divisible by R , we can turn it into one through the following correction step: We need to find some k such that $z - kN$ is divisible

²Note that \mathbb{Z}_N is *unordered*. We only talk about smallness of *representatives* of elements of \mathbb{Z}_N , not the elements of \mathbb{Z}_N themselves. In particular, one should not consider the multiplication by \underline{R}^{-1} as some form of scaling, but instead as an abstract permutation of \mathbb{Z}_N .

Algorithm 4 Montgomery reduction, implementation-view**Require:** N odd modulus, $R = 2^n > N$, $T \in \mathbb{Z}$ representative of $\overline{N^{-1}} \in \mathbb{Z}_R$ **Require:** $z \in \mathbb{Z}$ representative mod N , to be reduced**Ensure:** $\mathbf{mont}_N^+(z)$ representative of $\underline{zR^{-1}} \in \mathbb{Z}_N$ satisfying $|\mathbf{mont}_N^+(z)| \leq \frac{|z|}{2^n} + \frac{N}{2}$.

- 1: $\bar{k} \leftarrow \overline{zT}$ ▷ Unsigned single-width multiply
- 2: $k \leftarrow \bar{k} \bmod^\pm R$ ▷ Canonical signed representative
- 3: $c \leftarrow \lfloor \frac{kN}{R} \rfloor$ ▷ Signed multiply-high with truncation
- 4: $z_{\text{high}} = \lfloor \frac{z}{R} \rfloor$ ▷ High part extraction
- 5: $\mathbf{mont}_N^+(z) \leftarrow z_{\text{high}} - c$ ▷ Signed subtraction/addition

by R , that is, $\bar{z} = \overline{kN}$ in \mathbb{Z}_R . Since N and R are coprime, this is achieved by taking k to be a small representative of $\bar{z} \cdot \overline{N^{-1}}$ in \mathbb{Z}_R ; we will always choose $\bar{z}\overline{N^{-1}} \bmod^\pm R$.

The so obtained ‘‘Montgomery reduction’’ is summarized in [Algorithm 2](#) and denoted $\mathbf{mont}_N^+(z)$ – with R always being implicit. [Algorithm 2](#) also shows a close variant $\mathbf{mont}_N^-(z)$ which implements the correction step through an addition $z + kN$ instead of a subtraction: In this case, we want k to be a small representative of $-\bar{z} \cdot \overline{N^{-1}}$ in \mathbb{Z}_R , for which we choose $-\bar{z}\overline{N^{-1}} \bmod^\pm R$. We will call this variant ‘‘negative’’ Montgomery reduction. Their relation is as follows:

Fact 3. Assume the context of [Algorithm 2](#). If $\bar{z} \neq \overline{2^{n-1}} \in \mathbb{Z}_R$, then $\mathbf{mont}_N^+(z) = \mathbf{mont}_N^-(z)$. Otherwise, $\mathbf{mont}_N^-(z) = \mathbf{mont}_N^+(z) - N$.

Proof. This follows from [Fact 1](#) and the fact that $\overline{2^{n-1}} \cdot \bar{x} = \overline{2^{n-1}}$ for odd x . □

Remark 1. The exceptional case $\bar{z} = \overline{2^{n-1}}$ can be made explicit: $\mathbf{mont}_N^\pm(z) = \frac{z \pm 2^{n-1}N}{2^n}$.

Implementation considerations. We briefly summarize known implementation aspects of Montgomery reduction.

Firstly, in the context of [Algorithm 2](#) for $\mathbf{mont}_N^+(z)$, $z - c$ is divisible by R , and hence $\frac{z-c}{R} = \lfloor \frac{z}{R} \rfloor - \lfloor \frac{c}{R} \rfloor$. This allows to rewrite the algorithm in terms of single-width operations, as detailed in [Algorithm 4](#). This description does *not* apply to $\mathbf{mont}_N^-(z)$: This is because $\frac{z+c}{R}$ will usually introduce a carry-in from low-half to high-half as part of $z + c$, and this carry is lost in $\lfloor \frac{z}{R} \rfloor + \lfloor \frac{c}{R} \rfloor$. We will revisit this later.

Secondly, consider the use of Montgomery reduction for modular multiplication by constants: If $z = ab$ for single-width values $a, b \in \mathbb{Z}$, and b is known in advance, then $\bar{b} \cdot \overline{N^{-1}} \in \mathbb{Z}_R$ can be precomputed and leads to [Algorithm 5](#), the Montgomery reduction for products (a.k.a., ‘‘Montgomery Multiplication’’) with one known factor.

Finally, for microarchitectures with length-doubling (‘‘long’’) and non-doubling products, the optimal implementation varies depending on what instructions are available. For the Neon instruction set, please refer to [Section 3.2.5](#) and [Algorithm 14](#).

2.5 Fixed point arithmetic

Let $n \in \{16, 32\}$. The fixed-point interpretation of a single-width signed integer $a \in \{-2^{n-1}, -2^{n-1} + 1, \dots, 2^{n-1} - 1\}$ is the single-precision fractional value $\frac{a}{2^{n-1}} \in [-1, +1)$. Likewise, the fixed-point interpretation of a double-width signed integer a is the double-precision fractional value $\frac{a}{2^{2n-1}}$.

In this interpretation, the double-precision product of two single-precision fractional values corresponds to a *doubling long multiplication* on the corresponding signed integers: $\frac{a}{2^{n-1}} \cdot \frac{b}{2^{n-1}} = \frac{ab}{2^{2n-2}} = \frac{2ab}{2^{2n-1}}$. For this reason, doubling long multiplications are found in

Algorithm 5 Montgomery multiplication, implementation-view**Require:** N odd modulus, $R = 2^n > N$ **Require:** $a, b \in \mathbb{Z}$ representative mod N with $|a|, |b| < R$.**Require:** Precomputed $\overline{b_{\text{tw}}} = \overline{b} \cdot \overline{N}^{-1} \in \mathbb{Z}_R$.**Ensure:** $\mathbf{mont}_N^+(a, b)$ representative of $\overline{abR}^{-1} \in \mathbb{Z}_N$ satisfying $|\mathbf{mont}_N^+(a, b)| \leq \frac{|a||b|}{2^n} + \frac{N}{2}$.

- 1: $\overline{k} \leftarrow \overline{a} \cdot \overline{b_{\text{tw}}}$ ▷ Unsigned single-width multiply
- 2: $k \leftarrow \overline{k} \bmod^{\pm} R$ ▷ Canonical signed representative
- 3: $c \leftarrow \lfloor \frac{kN}{R} \rfloor$ ▷ Signed multiply-high with truncation
- 4: $z_{\text{high}} = \lfloor \frac{ab}{R} \rfloor$ ▷ Multiply-high
- 5: $\mathbf{mont}_N^+(a, b) \leftarrow z_{\text{high}} - c$ ▷ Signed subtraction

some ISAs supporting fixed point arithmetic: Neon offers SQDMULL, Helium offers VQDMULL, and SVE 2 offers QDMULL.

Similarly, single-precision approximations to the product of two single-precision fractional values correspond to a *doubling long multiplication returning high half* $\frac{a}{2^{n-1}} \cdot \frac{b}{2^{n-1}} = \frac{2ab}{2^{2n-1}} \approx \frac{\lfloor \frac{2ab}{2^{n-1}} \rfloor}{2^{n-1}}$, with flexibility in terms of the choice of approximation $\llbracket - \rrbracket$; common choices are *truncation* via $\lfloor - \rfloor$ and *rounding* to the nearest integer $\lfloor - \rfloor$. For this reason, ISAs supporting fixed point arithmetic offer instructions for doubling long multiplication returning high halves, often with separate variants for truncation and rounding: For example, Neon offers SQDMULH (truncating) and SQRDMULH (rounding), Helium offers VQ[R]DMULH, and SVE2 offers Q[R]DMULH. We note that Intel’s AVX2 includes VPMULHRSW but not a non-rounding variant.

Finally, ISAs supporting fixed-point arithmetic often offer multiply-accumulate-add or even multiply-accumulate-subtract variants for their single-precision fixed-point multiplications: Neon from Armv8.1-A onwards offers VQRDMLAH and VQRDMLSH, Helium offers VQ[R]DMLAH, and SVE2 offers QRDMLAH and QRDMLSH. Interpreted as integer operations, those correspond to doubling long multiplications returning (rounded/truncated) high half with accumulate add/subtract.

2.6 Number Theoretic Transform

In Kyber, Saber, and Dilithium, we need arithmetic in $\mathcal{R}_q = \mathbb{Z}_q[x]/\langle x^{256} + 1 \rangle$, a polynomial ring. Here $q = 3329 = 13 \cdot 2^8 + 1$ for Kyber, $q = 2^{13}$ for Saber, and $q = 2^{23} - 2^{13} + 1 = 8380417$ for Dilithium. More specifically, we need to perform a matrix-to-vector multiplication and inner products. All three will be developed in parallel after we switch to a modulus q' for Saber [CHK⁺21] so that the results are the same as for a computation over $\mathbb{Z}[x]/\langle x^{256} + 1 \rangle$.

Let $\mathbb{F} = \mathbb{F}_q$ for Dilithium and Kyber and $\mathbb{F} = \mathbb{F}_{q'}$ for Saber. From the CRT (Chinese Remainder Theorem) we have the ring isomorphism (Figure 1):

$$\mathbb{F}[x]/\langle x^{2n} - c^2 \rangle \cong \mathbb{F}[x]/\langle x^n - c \rangle \times \mathbb{F}[x]/\langle x^n + c \rangle;$$

$$\sum_{i=0}^{2n-1} f_i x^i \leftrightarrow \left(\sum_{i=0}^{n-1} (f_i + c f_{n+i}) x^i, \sum_{i=0}^{n-1} (f_i - c f_{n+i}) x^i \right).$$

To split a $2n$ -long polynomial, we perform CT butterflies between n pairs of coefficients, each from one half of the polynomial. Everything can be done in-place, and the CT butterfly has an obvious inverse — the GS butterfly, except for a factor of 2. For even n and $\pm c$ with square roots in \mathbb{F} we can recurse this process, each stage comprising the same number of butterflies. Let ζ be a principal root of order 2^k , so that $\zeta^{2^{k-1}} = -1$. An

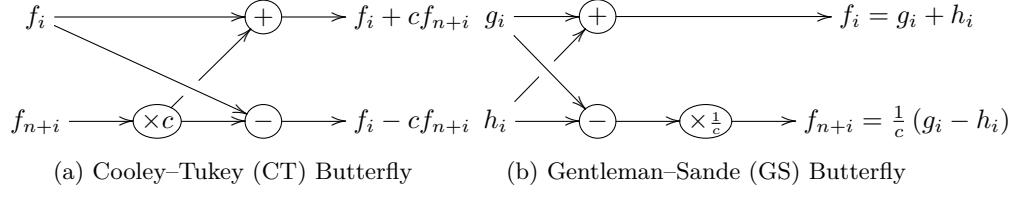


Figure 1: The “Butterflies” of Fast Fourier Transforms

(incomplete) NTT is defined as the series of ring isomorphisms computed as follows:

$$\begin{aligned}
& \frac{\mathbb{F}[x]}{\langle x^{d \cdot 2^k} - c^{2^k} \rangle} \cong \frac{\mathbb{F}[x]}{\langle x^{d \cdot 2^{k-1}} - c^{2^{k-1}} \rangle} \times \frac{\mathbb{F}[x]}{\langle x^{d \cdot 2^{k-1}} - \zeta^{2^{k-1}} c^{2^{k-1}} \rangle} \\
& \cong \frac{\mathbb{F}[x]}{\langle x^{d \cdot 2^{k-2}} - c^{2^{k-2}} \rangle} \times \frac{\mathbb{F}[x]}{\langle x^{d \cdot 2^{k-2}} - \zeta^{2^{k-1}} c^{2^{k-2}} \rangle} \times \\
& \quad \frac{\mathbb{F}[x]}{\langle x^{d \cdot 2^{k-2}} - \zeta^{2^{k-2}} c^{2^{k-2}} \rangle} \times \frac{\mathbb{F}[x]}{\langle x^{d \cdot 2^{k-2}} - \zeta^{3 \cdot 2^{k-2}} c^{2^{k-2}} \rangle} \\
& \cong \dots \cong \prod_{i=0}^{2^k-1} \frac{\mathbb{F}[x]}{\langle x^d - c \cdot \zeta^{\text{br}_k(i)} \rangle},
\end{aligned}$$

where $\text{br}_k((b_{k-1} \dots b_1 b_0)_2) := (b_0 b_1 \dots b_{k-1})_2$ (“ k -bit reversal”).

Here $k = 7$, $d = 2$, $c^{128} = -1$ for Kyber, $k = 8$, $d = 1$, $c^{256} = -1$ for Dilithium, and $\zeta = c^2$ for both, as the NTT is specified. Saber is flexible and only requires $d \cdot 2^k = 256$ and $c^{2^{k-1}} = -1$. The image under the ring isomorphism of a polynomial f is called “the NTT” of f and denoted $NTT(f)$. A polynomial product fg in the ring is computed as $fg = NTT^{-1}(NTT(f) \circ NTT(g))$, where \circ is the `base_mul` giving products in each of $\frac{\mathbb{F}[x]}{\langle x^d - c \cdot \zeta^{\text{br}_k(i)} \rangle}$.

3 Modular Multiplication

In this section, we present improvements to Barrett reduction and Montgomery multiplication from a theoretical and implementation perspective: In Section 3.1, we present a relation between Barrett reduction and Montgomery reduction and expand it to a relation between Montgomery multiplication and a new variant of modular multiplication via Barrett reduction which we call “Barrett multiplication”³. We also introduce two new variants of Montgomery multiplication using fixed-point arithmetic. In Section 3.2, we study implementations on SIMD extensions, focusing on the Neon instruction set. Concretely, we find a 3-instruction sequence for SIMD modular multiplication by known constants, improving on the 4-instruction sequence introduced by [Sei18, LS19], and a 5-instruction sequence for modular multiplication with unknown inputs on the Neon instruction set, improving the sequence used in [NG21]. We also describe a 4-instruction sequence for two unknown inputs; it does impose a parity constraint on the input, however, which may or may not be satisfiable depending on the application context.

3.1 Theory

3.1.1 Barrett reduction vs. Montgomery reduction

In this section, we compare Barrett and Montgomery reduction for single-width values.

³See Addendum: Related work for a post-publication correction with respect to prior art.

Proposition 1. Let N be odd, $R = 2^n > N$ and $z \in \mathbb{Z}$. Then Barrett reduction and negative Montgomery reduction satisfy the following relation:

$$\mathbf{bar}_N^\pm(z) = \mathbf{mont}_N^-(z(R \bmod^\pm N)). \quad (1)$$

More generally, for an arbitrary approximation $\llbracket \cdot \rrbracket$, we have

$$\mathbf{bar}_N^{\llbracket \cdot \rrbracket}(z) = \mathbf{mont}_N^-(z(R \bmod^{\llbracket \cdot \rrbracket} N))$$

Remark 2. Since $\mathbf{mont}_N^-(x)$ computes a representative of $\underline{x} \cdot \underline{R}^{-1}$ in \mathbb{Z}_N , the factor $R \bmod^\pm N$ in (1) does not come as a surprise. It also explains why $\mathbf{bar}_N^\pm(z)$ and $\mathbf{mont}_N^\pm(zR \bmod^\pm N)$ can only differ by a multiple of N . The value in Proposition 1 is in working with explicit representatives.

Remark 3. It follows from Fact 3 that Proposition 1 also holds for $\mathbf{mont}_N^+(z)$ except for the case $\bar{z} \cdot \overline{R \bmod^\pm N} = \overline{2^{n-1}}$, in which case $\mathbf{bar}_N^\pm(z) = \mathbf{mont}_N^+(z(R \bmod^\pm N)) - N$.

Lemma 1. In the context of Proposition 1, $\overline{\llbracket \frac{R}{N} \rrbracket} = \overline{-R \bmod^{\llbracket \cdot \rrbracket} N} \cdot \overline{N}^{-1}$ in \mathbb{Z}_R , hence

$$\llbracket \frac{R}{N} \rrbracket \bmod^\pm R = \left(-(R \bmod^{\llbracket \cdot \rrbracket} N) \cdot (\overline{N}^{-1} \bmod^\pm R) \right) \bmod^\pm R. \quad (2)$$

Lemma 1. We have $N \llbracket \frac{R}{N} \rrbracket = R - R \bmod^{\llbracket \cdot \rrbracket} N$ in \mathbb{Z} . Passing to \mathbb{Z}_R and multiplying by \overline{N}^{-1} proves the claim. Equation 2 follows by applying $_ \bmod^\pm R : \mathbb{Z}_R \rightarrow \mathbb{Z}$. \square

Proposition 1. The proof is mostly careful unraveling of definitions.

$$\begin{aligned} \mathbf{bar}_N^{\llbracket \cdot \rrbracket}(z) &\stackrel{\text{def}}{=} z - N \cdot \left\lfloor \frac{z \llbracket \frac{R}{N} \rrbracket}{R} \right\rfloor \stackrel{\text{def}}{=} z - N \frac{z \llbracket \frac{R}{N} \rrbracket - (z \llbracket \frac{R}{N} \rrbracket) \bmod^\pm R}{R} \\ &\stackrel{\text{Lemma 1}}{=} z - \frac{zN \llbracket \frac{R}{N} \rrbracket - N \left[-(z(R \bmod^{\llbracket \cdot \rrbracket} N)(\overline{N}^{-1} \bmod^\pm R)) \bmod^\pm R \right]}{R} \end{aligned}$$

Note that the right hand side of this expression already matches the correction term occurring in $\mathbf{mont}_N^-(z(R \bmod^{\llbracket \cdot \rrbracket} N))$. Next, we replace $\llbracket \frac{R}{N} \rrbracket = \frac{R - (R \bmod^{\llbracket \cdot \rrbracket} N)}{N}$ and obtain

$$\begin{aligned} \dots &= z - \frac{zN \frac{R - (R \bmod^{\llbracket \cdot \rrbracket} N)}{N} - N \left[-(z(R \bmod^{\llbracket \cdot \rrbracket} N)(\overline{N}^{-1} \bmod^\pm R)) \bmod^\pm R \right]}{R} \\ &= \frac{z(R \bmod^{\llbracket \cdot \rrbracket} N) + N \left[-z(R \bmod^{\llbracket \cdot \rrbracket} N)(\overline{N}^{-1} \bmod^\pm R) \bmod^\pm R \right]}{R} \\ &= \mathbf{mont}_N^-(z(R \bmod^{\llbracket \cdot \rrbracket} N)). \quad \square \end{aligned}$$

Corollary 1. In the context of Proposition 1,

$$|\mathbf{bar}_N^{\llbracket \cdot \rrbracket}(z)| \leq \frac{|z| \cdot |R \bmod^{\llbracket \cdot \rrbracket} N|}{R} + \frac{N}{2}$$

In particular, if $|z| < N$, and $N < \frac{R}{2}$, then $|\mathbf{bar}_N^{\llbracket \cdot \rrbracket}(z)| < N$.

Proof. The first part follows from Proposition 1 and the bound for Montgomery reduction. For the second, recall $|_ \bmod^{\llbracket \cdot \rrbracket} N| \leq N$. \square

3.1.2 Barrett multiplication

The relation between Barrett reduction and Montgomery reduction exhibited in the previous section raises the question of whether there is a natural extension to Montgomery multiplication, and what the analog on the Barrett side is. The answer turns out to be a variant of Barrett reduction for multiplication with known constants, which we describe in this section. While very natural in retrospect, the definitions and results are novel to the best of our knowledge.⁴

Recall (Section 2.4.1) the idea of Barrett reduction: To reduce $z \in \mathbb{Z}$, we approximate

$$z \bmod^{\pm} N = z - N \cdot \left\lfloor \frac{z}{N} \right\rfloor = z - N \cdot \left\lfloor \frac{z \frac{R}{N}}{R} \right\rfloor \approx z - N \cdot \left\lfloor \frac{z \left\lfloor \frac{R}{N} \right\rfloor}{R} \right\rfloor,$$

replacing $z \frac{R}{N}$ by the precomputed $z \left\lfloor \frac{R}{N} \right\rfloor$. If $z = ab$ for $a, b \in \mathbb{Z}$ and b a known constant, we can improve the quality of the approximation by pulling b into the approximation, approximating $ab \frac{R}{N} \approx a \left\lfloor \frac{bR}{N} \right\rfloor$, where $\left\lfloor \frac{bR}{N} \right\rfloor$ can be precomputed. We call this the ‘‘Barrett multiplication’’ of a, b and denote it $\mathbf{bar}_N^{\llbracket \cdot \rrbracket}(a, b)$, or $\mathbf{bar}_N^{\pm}(a, b)$ if $\llbracket \cdot \rrbracket = \lfloor \cdot \rfloor$. As before, the choice of R is implicit in the notation and to be understood from the context. We describe Barrett multiplication in Algorithm 6.

Algorithm 6 Barrett multiplication, abstract view

Require: N modulus, $R = 2^n > N$

Require: $b \in \mathbb{Z}$, $\left\lfloor \frac{bR}{N} \right\rfloor \in \mathbb{Z}$ precomputed integer approximation of $\frac{bR}{N}$.

Require: $a \in \mathbb{Z}$ representative mod N with $|a| < R$, to be reduced

Ensure: $\mathbf{bar}_N^{\llbracket \cdot \rrbracket}(a, b)$ representative of ab with $|\mathbf{bar}_N^{\llbracket \cdot \rrbracket}(a, b)| < N$.

- 1: $z \leftarrow ab$
 - 2: $t \leftarrow \left\lfloor \frac{a \left\lfloor \frac{bR}{N} \right\rfloor}{R} \right\rfloor$
 - 3: $c \leftarrow Nt$
 - 4: $\mathbf{bar}_N^{\llbracket \cdot \rrbracket}(a, b) \leftarrow z - c$
-

We now obtain the desired analog of Proposition 1 for Barrett multiplication:

Proposition 2. Let N be odd, $R = 2^n > N$ and $a, b \in \mathbb{Z}$. Then Barrett multiplication and negative Montgomery multiplication satisfy the following relation:

$$\mathbf{bar}_N^{\pm}(a, b) = \mathbf{mont}_N^{\mp}(a, bR \bmod^{\pm} N).$$

More generally, for an arbitrary approximation $\llbracket \cdot \rrbracket$, we have

$$\mathbf{bar}_N^{\llbracket \cdot \rrbracket}(a, b) = \mathbf{mont}_N^{\llbracket \cdot \rrbracket}(a, bR \bmod^{\llbracket \cdot \rrbracket} N).$$

Proof. Replace $R \bmod^{\llbracket \cdot \rrbracket} N$ by $bR \bmod^{\llbracket \cdot \rrbracket} N$ in the proof of Proposition 1. \square

Corollary 2. In the context of Proposition 2,

$$|\mathbf{bar}_N^{\llbracket \cdot \rrbracket}(a, b)| \leq \frac{a(bR \bmod^{\llbracket \cdot \rrbracket} N)}{R} + \frac{N}{2}$$

In particular, for $|a| < N$ and $N < \frac{R}{2}$ we have $|\mathbf{bar}_N^{\llbracket \cdot \rrbracket}(a, b)| < N$.

⁴See Addendum: Related work for a post-publication correction with respect to prior art.

Algorithm 7 Montgomery multiplication via doubling, abstract view**Require:** N odd modulus, $R = 2^n > N$ **Require:** $a, b \in \mathbb{Z}$ representative mod N with $|a|, |b| < R$.**Require:** Precomputed $T = \overline{N}^{-1} \in \mathbb{Z}_R$.**Ensure:** $\mathbf{mont}_N^\pm(a, b)$ representative of $\underline{abR}^{-1} \in \mathbb{Z}_N$ satisfying $|\mathbf{mont}_N^\pm(a, b)| \leq \frac{|a||b|}{2^n} + \frac{N}{2}$.

- 1: $z \leftarrow \lfloor \frac{2ab}{R} \rfloor$
- 2: $k \leftarrow abT \bmod^\pm R$
- 3: $c \leftarrow \lfloor \frac{2kN}{R} \rfloor$
- 4: $\mathbf{mont}_N^\pm(z) \leftarrow \frac{z-c}{2}$

Algorithm 8 Montgomery multiplication via rounding, abstract view**Require:** N odd modulus, $R = 2^n > N$ **Require:** $a, b \in \mathbb{Z}$ representative mod N with $|a|, |b| < \frac{R}{2}$, s.t. a or b is odd.**Require:** Precomputed $T = -\overline{N}^{-1} \in \mathbb{Z}_R$.**Ensure:** $\mathbf{mont}_N^\pm(a, b)$ representative of $\underline{abR}^{-1} \in \mathbb{Z}_N$ satisfying $|\mathbf{mont}_N^\pm(a, b)| \leq \frac{|a||b|}{2^n} + \frac{N}{2}$.

- 1: $z \leftarrow \lfloor \frac{2ab}{R} \rfloor$
- 2: $k \leftarrow abT \bmod^\pm R$
- 3: $c \leftarrow \lfloor \frac{2kN}{R} \rfloor$
- 4: $\mathbf{mont}_N^\pm(z) \leftarrow \frac{z+c}{2}$

3.1.3 Montgomery multiplication via doubling

Because of the doubling inherent in many fixed point instructions, the variant of Montgomery multiplication described in [Algorithm 7](#) will be useful.

Proposition 3. *Algorithm 7 is correct.*

Proof. By construction, $ab - kN$ is divisible by R . Hence, so is $2ab - 2kN$, and we get $\lfloor \frac{2ab}{R} \rfloor - \lfloor \frac{2kN}{R} \rfloor = \frac{2(ab-kN)}{R} = 2 \left(\lfloor \frac{ab}{R} \rfloor - \lfloor \frac{kN}{R} \rfloor \right)$. [Algorithm 7](#) thus yields the same result as Montgomery multiplication. \square

3.1.4 Montgomery multiplication via rounding

As first pointed out by Seiler in [\[Sei18\]](#) and mentioned in [Section 2.4.2](#), single-width Montgomery multiplication [Algorithm 5](#) breaks when trying to use addition instead of subtraction in the final step, because of a carry-in from low half to high half. [Algorithm 8](#) presents a remedy using rounding. Note the assumption that one of the inputs is odd.

Proposition 4. *Algorithm 8 is correct.*

Proof. Since we use $-\overline{N}^{-1} \in \mathbb{Z}_R$ instead of $\overline{N}^{-1} \in \mathbb{Z}_R$, we have $\overline{ab} = -\overline{kN}$ in \mathbb{Z}_R . Assuming $\overline{ab} \neq 2^{n-1}$, [Fact 1](#) therefore implies $ab \bmod^\pm R = -(kN \bmod^\pm R)$, and hence

$$\left\lfloor \frac{2ab}{R} \right\rfloor + \left\lfloor \frac{2kN}{R} \right\rfloor = \frac{2ab - (ab \bmod^\pm R) + 2kN - (kN \bmod^\pm R)}{R} = \frac{2(ab - kN)}{R}.$$

The result of [Algorithm 8](#) therefore equals that of ordinary Montgomery multiplication.

It remains to be justified why $\overline{ab} \neq 2^{n-1}$, which involves the assumption that either a or b are odd: If, say, b is odd, then $\overline{ab} = 2^{n-1}$ implies $\overline{a} = 2^{n-1}$, hence $|a| \leq 2^{n-1} = \frac{R}{2}$, contradicting the assumption that $|a|, |b| < \frac{R}{2}$. \square

3.2 Implementation

In this section, we look at Barrett and Montgomery multiplication from an implementation perspective, focusing on the Armv8-A version of the Neon SIMD instructions.

3.2.1 Barrett multiplication in 3-instructions

Analogously to [Algorithm 3](#), Barrett multiplication can be described in terms of single-width operations. The details are spelled out in [Algorithm 9](#). We see that Barrett multiplication can be expressed in terms of 3 single-width operations: $1 \times$ unsigned multiply-low, $1 \times$ unsigned multiply-low-accumulate, $1 \times$ multiply-high-with-rounding.

Algorithm 9 Barrett multiplication	Algorithm 10 Barrett multiplication in Neon
Require: N odd, $R = 2^n$ s.t. $N < \frac{R}{3}$. Require: $b \in \mathbb{Z}$, $\lfloor \frac{bR}{N} \rfloor \in \mathbb{Z}$ approx. $\frac{bR}{N}$. Require: $a \in \mathbb{Z}$, $ a \leq R$, to be multiplied Ensure: $z \equiv ab \pmod{N}$, $ z < \frac{3}{2}N < \frac{R}{2}$. 1: $\bar{z} \leftarrow \bar{a} \cdot \bar{b}$ 2: $t \leftarrow \lfloor a \lfloor \frac{bR}{N} \rfloor / R \rfloor$ 3: $\bar{z} \leftarrow \bar{z} + -\bar{N} \cdot \bar{t}$ 4: $\mathbf{bar}_{\frac{R}{N}}(a, b) = z \leftarrow \bar{z} \bmod^{\pm} R$	Require: N odd, $R = 2^n$ s.t. $N < \frac{R}{3}$. Require: $b \in \mathbb{Z}$, $\lfloor \frac{bR}{N} \rfloor_2$ precomputed Require: $a \in \mathbb{Z}$, $ a \leq R$, to be multiplied Ensure: $z \equiv ab \pmod{N}$, $ z < \frac{3}{2}N < \frac{R}{2}$. 1: $\mathbf{mul} \ z, \bar{a}, \bar{b}$ 2: $\mathbf{sqrddmulh} \ t, a, \lfloor \frac{bR}{N} \rfloor_2$ 3: $\mathbf{mls} \ z, t, \bar{N}$

In Neon, unsigned multiply-low and multiply-low-accumulate are implemented via `MUL` and `MLA`, respectively. The multiply-high-with-rounding operations $(a, b) \mapsto \lfloor \frac{ab}{2^n} \rfloor$ does not have an exact match in Neon, but as explained in [Section 2.5](#), there is `SQRDMULH` which computes $(a, b) \mapsto \lfloor \frac{2ab}{2^n} \rfloor$ instead. We work around this difference by choosing the even integer approximation $\lfloor \cdot \rfloor_2$ as the basis for Barrett multiplication: In this case, we have $\lfloor \frac{a \lfloor bR/N \rfloor_2}{R} \rfloor = \lfloor \frac{2a(\lfloor bR/N \rfloor_2/2)}{R} \rfloor$, which can be implemented through `SQRDMULH` since $\lfloor \frac{bR}{N} \rfloor_2/2$ can be computed upfront. We show the resulting Neon sequence in [Algorithm 10](#).

Note, however, that Barrett multiplication requires one factor to be known upfront. It does not apply for “point multiplication” of two unknown values.

Remark 4. This strategy works for 16- and 32-bit moduli, and any SIMD ISA which offers a double-multiply-high-with-rounding instruction. This includes the M-Profile Vector Extension (MVE), the Scalable Vector Extension 2 (SVE2) and, (16-bit lanes only), AVX2.

3.2.2 Barrett reduction

We comment on the implementation of Barrett reduction ([Algorithm 3](#)) in the Neon instruction set. For Barrett reduction of a single-width value, we choose R as large as possible in [Algorithm 3](#) so that $\lfloor \frac{R}{N} \rfloor$ is still a single-width signed value, increasing precision of the approximation. To compute $\lfloor \frac{z \lfloor \frac{R}{N} \rfloor}{R} \rfloor$, however, we can no longer use `SQRDMULH` as in [Algorithm 10](#) but have to split it into `SQDMULH` and a rounding right shift `SRSRHR`. We show our implementation of Barrett reduction in the Neon instruction set in [Algorithm 11](#).

Algorithm 12 Montgomery multiplication with doubling.

Require: N odd modulus, $R = 2^n > N$

Require: $a, b \in \mathbb{Z}$ representative mod N with $|a|, |b| < R$.

Require: Precomputed $T = \overline{N}^{-1} \in \mathbb{Z}_R$.

Ensure: $\mathbf{mont}_N^+(a, b)$ representative of $\underline{abR}^{-1} \in \mathbb{Z}_N$ satisfying $|\mathbf{mont}_N^+(a, b)| \leq \frac{|a||b|}{2^n} + \frac{N}{2}$.

- 1: sqdmulh z, a, b
 - 2: mul $k, a, bT \bmod^\pm R$
 - 3: sqdmulh c, k, N
 - 4: shsub z, z, c
-

Old Algorithm 11 Barrett Reduction (Vectorized) [NG21, Algorithm 13]

Require: Odd modulus N , i bits long.

Require: Radix $R = 2^{16}$ or 2^{32}

Require: Rounding constant $r = 2^{i-3}$.

Require: Multiplier $V = \lceil 2^{i-2}R/N \rceil$

Ensure: $z \equiv B \pmod{N}$, $\frac{-N}{2} \leq z < \frac{N}{2}$

- 1: smull T0, B, V
- 2: smull2 T1, B, V
- 3: uzp2 T0, T0, T1
- 4: add T1, r, T0
- 5: sshr T1, T1, $\#(i-2)$
- 6: mls z, T1, N

Algorithm 11 Barrett Reduction for Neon

Require: Odd modulus N , i bits long.

Require: Radix $R = 2^{16}$ or 2^{32}

Require: Multiplier $V = \lceil 2^{i-2}R/N \rceil$

Ensure: $z \equiv B \pmod{N}$, $\frac{-N}{2} \leq z < \frac{N}{2}$

- 1: sqdmulh T0, B, V
 - 2: srshr T1, T1, $\#(i-1)$
 - 3: mls z, T1, N
-

sqdmulh = doubling multiplication, high half

sshr = signed shift right

srshr = signed shift right with rounding

Note: N, V can be one lane of a Neon register

3.2.3 Montgomery multiplication via doubling

Ordinary Montgomery multiplication does not lend itself to a straightforward implementation in Neon because Neon does not offer a multiply-high instruction. This is the reason why e.g. [NG21] use the long multiply UMULL to implement Montgomery multiplication.

We propose to use the doubling multiply-high instruction QDMULH instead to implement Algorithm 7. Moreover, the final step $\mathbf{mont}_N^\pm(z) \leftarrow \frac{z-c}{2}$ can be implemented via the halving subtract instruction SHSUB.

The resulting Neon sequence is shown in Algorithm 12. It provides a 5-instruction sequence for Montgomery multiplication of two unknown values, and a 4-instruction sequence if one factor is a constant.

3.2.4 Montgomery multiplication via rounding

It is natural to try to merge the multiply-high and subtract step in Montgomery multiplication to shorten the modular multiplication sequence further. However, there is no plain multiply-high-accumulate instruction. Instead, MVE, SVE2 and the Armv8.1-A extension to Neon provide a multiply-high-accumulate-with-rounding instruction, which lends itself to an implementation of Algorithm 8 as shown in Algorithm 13. Like Barrett multiplication, this provides a 3-instruction sequence for modular multiplication with a known constant; unlike Barrett multiplication, however, it also applies to two unknown factors, provided one of them is known to be odd. While this is a strong condition, one has some leverage to reason about parity since the result of Algorithm 13 is always even. Note also that since sqrdmlah does not perform halving, Algorithm 13 computes a representative of $\underline{2abR}^{-1}$ instead of \underline{abR}^{-1} .

Algorithm 13 Montgomery multiplication with rounding.

```

1: sqrdmulh  $z, a, b$ 
2: mul  $k, a, -bN^{-1} \bmod^{\pm} R$ 
3: sqrdmlah  $z, k, N$ 

```

3.2.5 Montgomery multiplication in long arithmetic

Old Algorithm 14 Neon Montgomery multiplication [NG21, Alg. 12][SKS⁺21].

Inputs: $(a, b) = (a, b)$
Outputs: $c \equiv abR^{-1} \pmod{N}$, $|c| < N$

```

1: smull  $l, a, b$ 
2: smull2  $h, a, b$ 
3: uzp1  $t0, l, h$ 
4: uzp2  $t1, l, h$ 
5: mul  $c, t0, \overline{N}^{-1} \bmod^{\pm} R$ 
6: smull  $l, c, N$ 
7: smull2  $h, c, N$ 
8: uzp2  $t0, l, h$ 
9: sub  $c, t1, t0$ 

```

Algorithm 14 Our Neon Montgomery

Inputs: $(a, b) = (a, b)$
Outputs: $c = abR^{-1} \pmod{N}$, $|c| < N$

```

1: smull  $l, a, b$ 
2: smull2  $h, a, b$ 
3: uzp1  $t, l, h$ 
4: mul  $t, t, -\overline{N}^{-1} \bmod^{\pm} R$ 
5: smlal  $l, t, N$ 
6: smlal2  $h, t, N$ 
7: uzp2  $c, l, h$ 

```

Steps 3–7 do a better $l, h \rightarrow c$ Montgomery reduction than [NG21, Alg. 12, Steps 3–9].

We have so far focused on single-width implementations of Montgomery and Barrett multiplication. Those implementations, however, do not lend themselves well to applications which need to compute *sums* of modular multiplications: In this case, it is natural to reduce only once after the accumulation, rather than once after every product. Single-width modular multiplication cannot achieve this because it misses the carry-in between low and high parts. Instead, we need Montgomery multiplication using long products. We show an implementation of Montgomery multiplication in long arithmetic in [Algorithm 14](#).

After long pairwise products via `smull`, `smull2` from two vectors, we perform a Montgomery reduction by taking the lower halves (conveniently, with `uzp1`). This we multiply by the inverse of the modulus with `mul`. We multiply the modulus to the result and accumulate the long products with `smlal`, `smlal2`. Now we collate the Montgomery results in the top half happily with `uzp2`. The result is exactly right as in [Algorithm 14](#). As desired, we can accumulate several products before the Montgomery reduction (cf. [Section 4.2](#)).

4 Implementation

In this section, we fix $\mathbb{F} = \mathbb{F}_q$ for Dilithium and Kyber, and $\mathbb{F} = \mathbb{F}_{q'}$ for Saber. [Section 4](#) is organized as follows: In [Section 4.1](#), we describe our choices of butterflies for NTTs. [Section 4.2](#) introduces the asymmetric multiplication applicable to the `MatrixVectorMul` in Kyber and Saber. [Section 4.3](#) describes our findings on how interleaving can be applied for radix-2 NTTs on Cortex-A72.

4.1 Butterflies

In this section, we adopt a more architectural viewpoint of radix-2 NTTs.

The need for permutations in the NTTs. For vectorized implementations, an important consideration is the overhead of permuting data within vector registers. This is required

when the distance between the inputs of a butterfly is less than the size of a SIMD register. First, we notice that since each SIMD register in Neon is holding 16 bytes, any butterfly taking inputs at distance larger than 16 bytes doesn't require any permutation. Now we carefully look at the NTTs at each layer and number the layers from 0. After each layer, the distance for the butterfly inputs is halved. For Dilithium and Saber, we compute 32-bit NTTs for degree-255 polynomials. At the k th layer, we are computing butterflies with inputs distancing by $4 \cdot 2^{7-k} = \frac{512}{2^k}$ bytes. Therefore, after the 5th layer, any follow-up NTTs require permutations. As for Kyber with 16-bit NTTs for degree-255 polynomials, it is after the 4th layer that one needs permutations for the follow-up NTTs.

{ld, st}{1, 2, 3, 4} and trn{1, 2}. `ld{2, 3, 4}` are loading with the indicated degree of interleaving. An array of structures with 2 (3, 4) elements are loaded to 2 (3, 4) SIMD registers where the first lane of each register is holding the first structure and so on. On the other hand, `ld1` is simply loading consecutively to 1 to 4 SIMD registers. `st{1, 2, 3, 4}` are their counterparts for storing structures. Besides shuffling with memory operations, we have `trn{1, 2}` for permuting the elements of SIMD registers. `trn1` (`trn2`) moves the even (odd) indices of the first source to the even indices of the destination and the even (odd) indices of the second source to the odd indices of the destination.

Saber. First of all, since Armv8-A provides instructions for both 16-bit and 32-bit arithmetic, we find no reasons to employ 16-bit NTTs as in [NG21]. We decide to implement 32-bit NTT as implemented for Cortex-M4 in [CHK⁺21]. For NTT, we compute for $\mathbb{F}[x]/\langle x^{256} + 1 \rangle$ with 6 layers of CT butterflies. On the other hand, we compute NTT^{-1} for $\mathbb{F}[x]/\langle x^{256} - 1 \rangle$ with 6 layers of CT butterflies and then map $\mathbb{F}[x]/\langle x^{256} - 1 \rangle$ to $\mathbb{F}[x]/\langle x^{256} + 1 \rangle$. Recall that at the end of NTT^{-1} , we have to multiply each coefficient with 2^{-k} , so we can multiply each chunk of 4 coefficients with the precomputed $(2^{-k}, 2^{-k}\zeta^{-1}, 2^{-k}, \dots, 2^{-k}\zeta^{-63})$.

Dilithium. We implement NTT with CT butterflies and NTT^{-1} with GS butterflies. For NTT, after 4 radix-2 splits, the distance of the butterfly inputs for the next layer is 32 bytes. For the next 4 layers of NTTs, we first load with `ld1` and apply two layers of radix-2 splits on four SIMD registers as usual. Next, we transpose the four registers with Algorithm 29. At the end of butterflies, we can store with `st4` to cancel out the transpose. For the NTT^{-1} , we invert the entire process: for the initial 4 layers of NTT^{-1} , we load with `ld4`, compute two layers with GS, invert Algorithm 29, compute two layers with GS, and store with `st1`. For the last 4 layers, we invert CT butterflies with GS butterflies and merge half of the multiplications by 2^{-8} with ζ^{-128} .

Kyber. We also implement NTT with CT butterflies and NTT^{-1} with GS butterflies for Kyber. For the NTT, after 4 radix-2 splits, the distance of the butterfly inputs for the next layer is 16 bytes. Now we proceed for the bottom 3 layers with a different permutation. First, we `ld4` each 4-byte to 8 SIMD registers. Next, we use `trn1` and `trn2` to separate the upper 4-bytes from the lower 4-bytes for butterflies as shown in Algorithm 30. In this way, we can then apply 3 layers of butterflies without intermediate permutations, which prohibits an aggressive interleaving of instructions. We will discuss the interleaving in Section 4.3. For NTT^{-1} , we invert the entire NTT and also merge half of the multiplications by 2^{-7} with ζ^{-64} .

Table 3 is the summary of butterflies for NTT and NTT^{-1} .

Table 3: Summary of butterflies for NTTs and NTT^{-1} s.

	NTT	NTT^{-1}
kyber	4-layer-CT + 3-layer-CT	3-layer-GS + 4-layer-GS
saber	$2 \times$ 3-layer-CT	$2 \times$ 3-layer-CT
dilithium	$2 \times$ 4-layer-CT	$2 \times$ 4-layer-GS

4.2 Asymmetric Multiplication

We introduce an idea that we call *asymmetric multiplication* for improving the efficiency of matrix-to-vector polynomial multiplication based on incomplete NTTs, and in general whenever incomplete NTTs are cached. It is thus applicable to Kyber and Saber, but not to Dilithium.

Recall that for Kyber and Saber, we can compute As' as $\text{NTT}^{-1}(\text{NTT}(A) \circ \text{NTT}(s'))$, where $k = 2$ and 4 for Kyber and Saber, respectively. As with any matrix-to-vector product, every entry of $\text{NTT}(s')$ will be multiplied with ℓ entries from $\text{NTT}(A)$. It is therefore beneficial to cache $\text{NTT}(s')$, which is indeed a known and common optimization technique for NTT-based multiplication. Asymmetric multiplication extends this observation by caching more computations on the multiplicands of one side.

Specifically, note that when computing the product of $a = \sum_i a_i x^i$ and $s = \sum_i s_i x^i$ in $\mathbb{F}[x]/\langle x^k - \omega \rangle$, we need to compute and sum $a_i s_j$ for $i + j < k$ and $\omega a_i s_j = a_i (\omega s_j)$ for $i + j \geq k$. It is therefore beneficial to precompute and cache the scaled ωs along with s . After the precomputation, the arithmetic cost for products in $\mathbb{F}[x]/\langle x^k - \omega \rangle$ is then effectively reduced to that of products in $\mathbb{F}[x]/\langle x^k - 1 \rangle$. Note that this is different from the isomorphism $\mathbb{F}[x]/\langle x^k - \omega \rangle \cong \mathbb{F}[y]/\langle y^k - 1 \rangle$, which doesn't work for Kyber as there is no k -th roots for ω . We call the multiplication strategy “asymmetric” because it requires the s -input in expanded form $(s, \omega s)$, while the a -input in the usual form. Algorithm 16 is an illustration. Note again the arithmetical similarity between Algorithm 15 and Algorithm 16.

We denote `NTT_heavy` the composition of the incomplete NTT with the computation $s \mapsto (s, \omega s)$, and `asymmetric_mul` implementing `asymmetric_mul(NTT(a), NTT_heavy(s)) = NTT(a) \circ NTT(s)` in the asymmetric fashion. Then As' can be computed as

$$As' = \text{NTT}^{-1}(\text{asymmetric_mul}(\text{NTT}(A), \text{NTT_heavy}(s'))).$$

Lastly, we extend the idea of *better accumulation for schoolbook multiplication* in [CHK⁺21] to *better accumulation for asymmetric multiplication*, giving the 64-bit results and reducing them to 32-bit after computing all the corresponding asymmetric multiplications. See Algorithm 33.

Algorithm 15 4×4 convolution.**Inputs:** $c, l, h, a_0, \dots, a_3, T_0, \dots, T_3$ **Output:**

$$c_0 + c_1x + c_2x^2 + c_3x^3 =$$

$$(\mathbf{a} * \mathbf{b}) \mathbb{R}^{-1} \bmod (x^4 - 1)$$

- 1: Name $\mathbf{c} = c_0,$
 $(\mathbf{a}_0, \dots, \mathbf{a}_3) = (a_0, a_1, a_2, a_3),$
 $(T_0, \dots, T_3) = (b_0, b_1, b_2, b_3)$
- 2: `smull1 l, a0, T0`
- 3: `smull12 h, a0, T0`
- 4: `smlal1 l, a1, T3`
- 5: `smlal12 h, a1, T3`
- 6: `smlal1 l, a2, T2`
- 7: `smlal12 h, a2, T2`
- 8: `smlal1 l, a3, T1`
- 9: `smlal12 h, a3, T1`
- 10: `q_montgomery c, l, h`
- 11: Rename $(T_0-3) = (b_1, b_2, b_3, b_0),$
 $\mathbf{c} = c_1$ and repeat lines 4–10
- 12: Rename $(T_0-3) = (b_2, b_3, b_0, b_1),$
 $\mathbf{c} = c_2$ and repeat lines 4–10
- 13: Rename $(T_0-3) = (b_3, b_0, b_1, b_2),$
 $\mathbf{c} = c_3$ and repeat lines 4–10

Algorithm 16 4×4 asymmetric multiplication.**Inputs:** $c, l, h, a_0, \dots, a_3, T_0, \dots, T_3$ **Output:**

$$c_0 + c_1x + c_2x^2 + c_3x^3 = (\mathbf{a} * \mathbf{b}) \mathbb{R}^{-1} \bmod (x^4 - \omega)$$

- 1: Name $\mathbf{c} = c_0,$
 $(\mathbf{a}_0, \dots, \mathbf{a}_3) = (a_0, a_1, a_2, a_3),$
 $(T_0, \dots, T_3) = (b_0, \omega b_1, \omega b_2, \omega b_3)$
- 2: `smull1 l, a0, T0`
- 3: `smull12 h, a0, T0`
- 4: `smlal1 l, a1, T3`
- 5: `smlal12 h, a1, T3`
- 6: `smlal1 l, a2, T2`
- 7: `smlal12 h, a2, T2`
- 8: `smlal1 l, a3, T1`
- 9: `smlal12 h, a3, T1`
- 10: `q_montgomery c, l, h`
- 11: Rename $(T_0-3) = (b_1, \omega b_2, \omega b_3, b_0),$ $\mathbf{c} = c_1$
and repeat lines 4–10
- 12: Rename $(T_0-3) = (b_2, \omega b_3, b_0, b_1),$ $\mathbf{c} = c_2$
and repeat lines 4–10
- 13: Rename $(T_0-3) = (b_3, b_0, b_1, b_2),$ $\mathbf{c} = c_3$
and repeat lines 4–10

`q_montgomery` is Step 3–7 in Algorithm 14.

4.3 Interleaving for Multi-Layer Butterflies on Cortex-A72

This section describes our findings on how to implement radix-2 NTTs for the CPU Cortex-A72. We follow the software optimization guide of Cortex-A72 [ARM].

In-order frontend and out-of-order backend. In the in-order frontend of the pipeline, instructions are fetched and decoded into internal micro-operations (μops). After renaming the registers, μops are dispatched to the out-of-order backend. In the backend, there is one branch pipeline B, two integer pipelines I0 and I1, one integer multi-cycle pipeline M, two FP/ASIMD pipelines F0 and F1, one load pipeline L, and one store pipeline S. While up to three μops can be dispatched per cycle, there are limitations on the number of each type of μops that can be dispatched simultaneously. The following are the numbers for each type in a single cycle: one μop using B, up to two μops using I0/I1, up to two μops using M, one μop using F0, one μop using F1, and up to two μops using L/S. Furthermore, μops are dispatched in the oldest-to-youngest age order.

F0 and F1 for butterflies. We focus on the pipelines F0 and F1 for our vectorized implementation. The basic building blocks for butterflies are Algorithm 17 and Algorithm 18. Instructions `mul`, `mls`, `sqrddmulh` can only go to F0, while `sub` and `add` go to F0 or F1. We interleave the instructions so `sub` and `add` have a better chance to be dispatched to F1. We believe F0 is the bottleneck of NTTs, and hence, reducing the loading of F0 speeds up the computation.

Algorithm 17 CT butterflies.**Inputs:**

$$a, b, t, (z[1], z[h]) = (\bar{\omega}, \lfloor \frac{\omega^R}{2} \rfloor_2)$$

Outputs:

$$(a, b) = (a + \omega b, a - \omega b)$$

- 1: mul t, b, z[h]
- 2: sqrdmulh b, b, z[1]
- 3: mls t, b, N
- 4: sub b, a, t
- 5: add a, a, t

Algorithm 18 GS butterflies.**Inputs:**

$$a, b, t, (z[1], z[h]) = (\bar{\omega}, \lfloor \frac{\omega^R}{2} \rfloor_2)$$

Outputs:

$$(a, b) = (a + b, (a - b)\omega)$$

- 1: sub t, a, b
- 2: add a, a, b
- 3: mul b, t, z[h]
- 4: sqrdmulh t, t, z[1]
- 5: mls b, t, N

qq_butterfly_{top, bot} and qq_butterfly_mixed{, _rev}. To facilitate the development of assembly implementation of radix-2 NTTs with interleaving, we split the computation of each layer into two `qq_butterfly_top` and two `qq_butterfly_bot`. `qq_butterfly_top` computes 4 Montgomery multiplications and `qq_butterfly_bot` computes 4 sub-add pairs as shown in [Algorithm 34](#) and [Algorithm 35](#). They are designed in the way that if we pass the same arguments to them, calling `qq_butterfly_top` followed by `qq_butterfly_bot` implements CT butterflies and reversing the order implements GS butterflies. [Algorithm 38](#) is a straightforward implementation of a 4-layer-CT-butterfly. If there are no dependencies, we can interleave `qq_butterfly_bot` with `qq_butterfly_top` giving `qq_butterfly_mixed` for CT butterflies and `qq_butterfly_mixed_rev` for GS butterflies as shown in [Algorithm 36](#) and [Algorithm 37](#).

Multi-layer butterflies. A common approach for reducing the number of memory operations is to compute several layers of NTTs at a time with multi-layer butterflies. To avoid the dependencies when interleaving instructions, we find that for radix-2 NTTs, computing coefficients distributed over 16 SIMD registers is the most beneficial approach. This suggests that 4 layers at a time are possible since $2^4 = 16$.

Interleaving for multi-layer butterflies. At first glance, it seems natural to compute the butterflies in the order $(v_0, v_8), \dots, (v_6, v_{14}), (v_1, v_9), \dots, (v_7, v_{15})$ for the 0th layer, $(v_0, v_4), (v_2, v_6), (v_8, v_{12}), (v_{10}, v_{14}), (v_1, v_5), (v_3, v_7), (v_9, v_{13}), (v_{11}, v_{15})$ for the 1st layer, and so on. Since the independencies of the first three layers are exploited, the computation can be interleaved as follows: interleave the first half of sub-add pairs of layer 0 with the second half of multiplications of layer 0, the second half of sub-add pairs of layer 0 with the first half of multiplications of layer 1, and so on. However, we cannot interleave layers 2 with 3 at all. To overcome this, we compute the butterflies in the following order: $(v_1, v_9), \dots, (v_7, v_{15}), (v_0, v_8), \dots, (v_6, v_{14})$ for the 0th layer, $(v_1, v_5), (v_3, v_7), (v_9, v_{13}), (v_{11}, v_{15}), (v_0, v_4), (v_2, v_6), (v_8, v_{12}), (v_{10}, v_{14})$ for the 1st layer, $(v_1, v_3), (v_5, v_7), (v_9, v_{11}), (v_{13}, v_{15}), (v_0, v_2), (v_4, v_6), (v_8, v_{10}), (v_{12}, v_{14})$ for the 2nd layer, and finally $(v_0, v_1), (v_2, v_3), (v_4, v_5), (v_6, v_7), (v_8, v_9), (v_{10}, v_{11}), (v_{12}, v_{13}), (v_{14}, v_{15})$ for the 3rd layer. In this order, we are exploiting the independencies among the entire 4-layer computation as shown in [Algorithm 19](#).

Algorithm 19 4 layers of interleaved 32-bit CT butterflies over 32 SIMD registers.

Inputs: $(v_0, \dots, v_{15}) = (a_0, \dots, a_{15})$

Outputs: $(v_0, \dots, v_{15}) = \text{NTT}(a_0, \dots, a_{15})$

Auxiliary registers: $v_{16}, \dots, v_{19}, v_{28}, \dots, v_{31}$

Twiddle factors:

$$\left\{ \begin{array}{l} v_{20} = h_0 \parallel 10 \parallel 0 \parallel Q, \quad v_{21} = h_2 \parallel 12 \parallel h_1 \parallel 11 \\ v_{22} = h_4 \parallel 14 \parallel h_3 \parallel 13, \quad v_{23} = h_6 \parallel 16 \parallel h_5 \parallel 15 \\ v_{24} = h_8 \parallel 18 \parallel h_7 \parallel 17, \quad v_{25} = h_{10} \parallel 110 \parallel h_9 \parallel 19 \\ v_{26} = h_{12} \parallel 112 \parallel h_{11} \parallel 111, \quad v_{27} = h_{14} \parallel 114 \parallel h_{13} \parallel 113 \end{array} \right.$$

Symbols:

$L0_0 = v_0, v_2, v_4, v_6, v_8, v_{10}, v_{12}, v_{14}$

$L0_1 = v_1, v_3, v_5, v_7, v_9, v_{11}, v_{13}, v_{15}$

$L1_0 = v_0, v_2, v_8, v_{10}, v_4, v_6, v_{12}, v_{14}$

$L1_1 = v_1, v_3, v_9, v_{11}, v_5, v_7, v_{13}, v_{15}$

$L2_0 = v_0, v_4, v_8, v_{12}, v_2, v_6, v_{10}, v_{14}$

$L2_1 = v_1, v_5, v_9, v_{13}, v_3, v_7, v_{11}, v_{15}$

$L3_0 = v_0, v_2, v_4, v_6, v_1, v_3, v_5, v_7$

$L3_1 = v_8, v_{10}, v_{12}, v_{14}, v_9, v_{11}, v_{13}, v_{15}$

$T0 = v_{16}, v_{17}, v_{18}, v_{19}$

$T1 = v_{28}, v_{29}, v_{30}, v_{31}$

$\text{mod} = v_{20}$

$W0 = v_{20}, 2, 3, v_{20}, 2, 3, v_{20}, 2, 3, v_{20}, 2, 3$

$W1 = v_{21}, 0, 1, v_{21}, 0, 1, v_{21}, 2, 3, v_{21}, 2, 3$

$W2 = v_{22}, 0, 1, v_{22}, 2, 3, v_{23}, 0, 1, v_{23}, 2, 3$

$W3_0 = v_{24}, 0, 1, v_{24}, 2, 3, v_{25}, 0, 1, v_{25}, 2, 3$

$W3_1 = v_{26}, 0, 1, v_{26}, 2, 3, v_{27}, 0, 1, v_{27}, 2, 3$

- 1: qq_butterfly_top L0_1, T0, mod, W0
 - 2: qq_butterfly_mixed L0_1, T0, L0_0, T1, mod, W0, W0
 - 3: qq_butterfly_mixed L0_0, T1, L1_1, T0, mod, W0, W1
 - 4: qq_butterfly_mixed L1_1, T0, L1_0, T1, mod, W1, W1
 - 5: qq_butterfly_mixed L1_0, T1, L2_1, T0, mod, W1, W2
 - 6: qq_butterfly_mixed L2_1, T0, L2_0, T1, mod, W2, W2
 - 7: qq_butterfly_mixed L2_0, T1, L3_0, T0, mod, W2, W3_0
 - 8: qq_butterfly_mixed L3_0, T0, L3_1, T1, mod, W3_0, W3_1
 - 9: qq_butterfly_bot L3_1, T1, mod, W3_1
-

5 Result

We provide benchmarking results on the Arm Cortex-A72 processor and the Apple M1.

Arm Cortex-A72. The Arm Cortex-A72 CPU implements the Armv8-A architecture and has a triple-issue out-of-order pipeline. Specifically, we use the Raspberry Pi 4 Model B featuring the quad-core Broadcom BCM2711 chipset. It comes with a 32 kB L1 data cache, a 48 kB L1 instruction cache, and a 1 MB L2 cache and runs at 1.5 GHz. For hashing, we use the SHA-3/SHAKE Neon implementation by Nguyen et al. [NG21]. For benchmarking individual functions we make use of the cycle counter of the PMU. For benchmarking the full cryptographic schemes, we use SUPERCOP.⁵ We use gcc version 10.3.0 with `-O3`.

⁵<https://bench.cr.yp.to/supercop.html>, Version 20210604

Table 4: Performance results for NTT, NTT_heavy, base_mul, and NTT⁻¹ for kyber768, saber, and dilithium3 on Cortex-A72 and Apple M1. dim refers to the module dimension. Some implementations implement the base_mul for each polynomial separately, while we implement it for an entire vector such that we can better optimize the accumulation. On Cortex-A72, we report the median cycle count of 10 000 executions. On Apple M1, we report the average cycle count of 10 000 executions. We also list related work on Cortex-A72, Cortex-A75, and Apple M1 for comparison.

Arm Cortex-A72 (Arm Cortex-A75 for [SKS ⁺ 21])						
		NTT	NTT_heavy	dim × base_mul	NTT ⁻¹	CRT
kyber768 (Ours)	A72	1 200	1 434	952	1 338	–
kyber768 [NG21]	A72	1 473 ^a	–	3 040 ^d	1 661	–
kyber768 [SKS ⁺ 21]	A75	2 332	–	3 × 1 313	3 209	–
saber 32-bit (Ours)	A72	1 529	2 031	2 689	1 896	–
saber 16-bit [NG21]	A72	1 991 ^b	–	1 500 ^d	1 893	813 ^d
dilithium3 (Ours)	A72	2 241	–	1 378	2 821	–
dilithium3 (ref)	A72	9 302	–	5 × 2 325	11 633	–
Apple M1						
		NTT	NTT_heavy	dim × base_mul	NTT ⁻¹	CRT
kyber768 (Ours)	M1	263	309	198	262	–
kyber768 [NG21]	M1	413 ^a	–	753 ^d	428	–
saber (Ours)	M1	301	411	790	389	–
saber 16-bit [NG21]	M1	539 ^c	–	380 ^d	531	206 ^d
dilithium3 (Ours)	M1	479	–	258	582	–
dilithium3 (ref)	M1	2 865	–	5 × 794	3 749	–

^a [NG21] reports cycles without a final reduction, while our implementation includes a reduction.

^b A fair comparison to our 32-bit NTT is 2 × 16-bit NTT + CRT = 4 795

^c A fair comparison to our 32-bit NTT is 2 × 16-bit NTT + CRT = 1 284

^d Our own benchmarks; not reported in [NG21].

Apple M1. The Apple M1 system-on-chip is contained in Apple’s 2020 MacBooks. It has four high-performance *Firestorm* cores, and four energy-efficient *Icestorm* cores. The Apple M1 has special instructions for Keccak. We use the Keccak implementation by Westerbaan [Wes] which makes use of these instructions. For obtaining cycle counts we make use of `m1cycles.c`⁶ from [NG21]. Due to the large and varying overhead of obtaining cycles, we cannot reasonably benchmark a single execution of a small function. Instead, we benchmark many iterations and report the average. We use clang version 12.0.5 with `-O3`.

Results for NTT and NTT⁻¹. Table 4 summarizes our results for the NTT for the level three parameter sets. On the Cortex-A72, we outperform the kyber768 NTT and NTT⁻¹ by Nguyen et al. [NG21] by 19% each, even though we include Barrett reduction which is not reported by Nguyen et al. [NG21]. Compared to the implementation by Sanal et al. [SKS⁺21], the speed-up is even more pronounced at 1.9× for the NTT and 2.4× for NTT⁻¹. For *saber*, our 32-bit NTT is 23% faster than the 16-bit NTT by Nguyen et al. [NG21]. However, the 16-bit NTT approach requires two NTTs followed by CRT and, consequently, our real speed-up is 3.1×. On the Apple M1, our speed-up compared to the kyber768 NTT and NTT⁻¹ by Nguyen et al. [NG21] is 1.6× each. The 16-bit *saber* NTTs are outperformed by our 32-bit NTTs by 44% and 27% on the M1. The actual speed-up when comparing the 32-bit NTT to two 16-bit NTTs followed by CRT is 4.3×. For Dilithium, we obtain a vast speed-up over the reference implementation.

⁶https://github.com/GMUCERG/PQC_NEON/blob/main/neon/kyber/m1cycles.c

Table 5: Cycle counts for `MatrixVectorMul` (MV), and `InnerProd` (IP) for `kyber768`, `saber`, and `dilithium3` on Cortex-A72 and Apple M1. For `kyber768` and `saber` the `InnerProd` in encapsulation (E) can re-use intermediate results from the `MatrixVectorMul`; in decapsulation (D) a full `InnerProd` is needed. `dilithium3` does not use an `InnerProd`. On Cortex-A72, we report median cycle count of 10 000 executions. On Apple M1, we report the average cycle count of 10 000 executions.

	Arm Cortex-A72			Apple M1		
	MV	IP(E)	IP (D)	MV	IP (E)	IP (D)
<code>kyber512</code> (Ours)	6 849	2 000	4 844	1 431	412	926
<code>kyber512</code> [NG21]	10 700	–	7 100	2 809	–	1 858
<code>kyber768</code> (Ours)	11 077	2 242	6 518	2 291	461	1 232
<code>kyber768</code> [NG21]	19 300	–	9 900	4 910	–	2 545
<code>kyber1024</code> (Ours)	16 338	2 758	8 487	3 247	509	1 536
<code>kyber1024</code> [NG21]	–	–	–	7 651	–	3 271
<code>lightsaber 32-bit NTT</code> (Ours)	18 149	7 038	11 113	3 933	1 556	2 376
<code>lightsaber 16-bit NTT</code> [NG21]	37 000	–	22 500	10 077	–	6 117
<code>lightsaber Toom-Cook</code> [NG21]	40 200	–	18 100	6 640	–	3 184
<code>saber 32-bit NTT</code> (Ours)	35 730	9 284	15 452	7 480	2 082	3 313
<code>saber 16-bit NTT</code> [NG21]	71 300	–	31 500	18 931	–	8 470
<code>saber Toom-Cook</code> [NG21]	81 000	–	25 000	14 029	–	4 345
<code>firesaber 32-bit NTT</code> (Ours)	56 109	11 783	20 112	12 074	2 608	4 248
<code>firesaber 16-bit NTT</code> [NG21]	–	–	–	30 393	–	10,839
<code>firesaber Toom-Cook</code> [NG21]	–	–	–	21 591	–	5 318
<code>dilithium2</code> (Ours)	26 268	–	–	5 316	–	–
<code>dilithium2</code> (ref)	135 182	–	–	45 742	–	–
<code>dilithium3</code> (Ours)	38 107	–	–	7 938	–	–
<code>dilithium3</code> (ref)	215 503	–	–	72 516	–	–
<code>dilithium5</code> (Ours)	54 759	–	–	11 353	–	–
<code>dilithium5</code> (ref)	334 865	–	–	118 211	–	–

Results for `MatrixVectorMul` and `InnerProd`. Table 5 presents the results for the core arithmetic operations `MatrixVectorMul` and `InnerProd` for all parameter sets. For `kyber768`, our `MatrixVectorMul` is $1.7\times$ faster on Cortex-A72 and $2.1\times$ faster on Apple M1 than previous implementations [NG21]. For `InnerProd`, our code is $1.5\times$ faster on Cortex-A72 and $2.1\times$ faster on Apple M1. For `saber`, we speed up `MatrixVectorMul` by $2.0\times$ on Cortex-A72 and $1.9\times$ on Apple M1. The speed-up for `InnerProd` is $1.6\times$ on Cortex-A72 and $1.3\times$ on Apple M1. Also note that for the `InnerProd` in encapsulation of Kyber and Saber, one can re-use `NTT_heavy(s')` to obtain a much faster `InnerProd`.

Results for full schemes. Table 6 shows our results for the full cryptographic schemes. Kyber runs 9 – 14% faster on Cortex-A72 and 26% – 41% faster on Apple M1 than previous work [NG21]. For Saber, the speed-ups are even more significant with 24 – 35% fewer cycles on Cortex-A72 and 19 – 36% fewer cycles on Apple M1. Unsurprisingly, our Dilithium implementation performs much better than the reference implementation.

On Saber’s SHA-3 performance. As we make use of a vectorized SHA-3 implementation computing two Keccak permutations at once, optimal performance can only be achieved if SHA-3/SHAKE calls can be parallelized. Unfortunately, the Saber specification mandates sampling vectors and matrices as a single call to SHAKE and can, thus, not benefit from

Table 6: Performance results for the full schemes `kyber768`, `saber`, and `dilithium3` on Cortex-A72 and Apple M1. On Cortex-A72, we report the median cycle count of 10 000 executions for Kyber and Saber, and 100 000 executions for Dilithium. On Apple M1, we report the average cycle count of 10 000 executions for Kyber and Saber, and 1 000 000 executions for Dilithium. For Dilithium, we sign 59-byte messages.

	Cortex-A72			Apple M1		
	K	E	D	K	E	D
<code>kyber512</code> (Ours)	62 459	80 710	76 443	14 939	24 834	20 893
<code>kyber512</code> [NG21]	67 903 ^a	88 906 ^a	87 563 ^a	23 000	32 500	29 400
<code>kyber512</code> [SKS+21] ^b	84 728	109 668	108 646	–	–	–
<code>kyber768</code> (Ours)	99 201	127 453	120 665	23 756	36 284	31 047
<code>kyber768</code> [NG21]	110 784 ^a	141 312 ^a	138 984 ^a	36 300	49 200	45 700
<code>kyber768</code> [SKS+21] ^b	143 791	180 687	179 085	–	–	–
<code>kyber1024</code> (Ours)	156 694	192 280	184 161	33 024	48 925	44 000
<code>kyber1024</code> [NG21]	176 809 ^a	215 665 ^a	214 076 ^a	55 900	71 600	67 100
<code>kyber1024</code> [SKS+21] ^b	228 082	272 418	270 668	–	–	–
<code>lightsaber</code> (Ours)	64 181	87 272	92 813	20 137	29 731	28 551
<code>lightsaber</code> [NG21] ^c	83 960 ^a	118 583 ^a	136 203 ^a	31 200	37 200	35 300
<code>saber</code> (Ours)	109 192	140 103	147 925	32 865	44 917	44 074
<code>saber</code> [NG21] ^c	158 757 ^a	206 337 ^a	226 304 ^a	51 300	59 900	58 000
<code>firesaber</code> (Ours)	175 104	211 382	222 317	50 345	65 402	64 593
<code>firesaber</code> [NG21] ^c	245 249 ^a	304 128 ^a	330 750 ^a	77 000	87 900	86 700
	K	S	V	K	S	V
<code>dilithium2</code> (Ours)	269 724	649 230	272 824	71 061	224 125	69 792
<code>dilithium2</code> (ref)	410 312	1 353 753	449 633	187 842	741 140	199 615
<code>dilithium3</code> (Ours)	515 776	1 089 387	447 460	152 435	365 248	104 821
<code>dilithium3</code> (ref)	743 166	2 308 598	728 866	358 848	1 218 027	329 187
<code>dilithium5</code> (Ours)	782 752	1 436 988	764 886	178 137	426 635	167 489
<code>dilithium5</code> (ref)	1 151 504	2 903 604	1 198 723	544 833	1 531 067	557 696

^a We re-benchmark the code from [NG21] in SUPERCOP.

^b [SKS+21] targets the Arm Cortex-A75.

^c Fastest implementation in [NG21] (Toom–Cook).

Keccak parallelization. We believe that the Saber specification should be changed. Saber’s performance on Cortex-A72 and Apple M1 will then be much closer to Kyber.

Acknowledgments

The authors in Taiwan thank the Ministry of Science and Technology for grant 109-2221-E-001-009-MY3, the Sinica Investigator Award AS-IA-109-M01, the Executive Yuan Data Safety and Talent Cultivation Project (AS-KPQ-109-DSTCP), and the Cybersecurity Center of Excellence Project at National Applied Research Labs.

References

- [AASA+20] Gorjan Alagic, Jacob Alperin-Sheriff, Daniel Apon, David Cooper, Quynh Dang, John Kelsey, Yi-Kai Liu, Carl Miller, Dustin Moody, Rene Peralta, Ray Perlner, Angela Robinson, and Daniel Smith-Tone. NISTIR8309 – status

- report on the second round of the nist post-quantum cryptography standardization process, July 2020. <https://doi.org/10.6028/NIST.IR.8309>.
- [ABCG20] Erdem Alkim, Yusuf Alper Bilgin, Murat Cenk, and François Gérard. Cortex-M4 optimizations for $\{R, M\}$ LWE schemes. *IACR Trans. Cryptogr. Hardw. Embed. Syst.*, 2020(3):336–357, 2020. <https://doi.org/10.13154/tches.v2020.i3.336-357>.
- [ABD⁺20a] Roberto Avanzi, Joppe Bos, Léo Ducas, Eike Kiltz, Tancrede Lepoint, Vadim Lyubashevsky, John M. Schanck, Peter Schwabe, Gregor Seiler, and Damien Stehlé. CRYSTALS–Dilithium. Submission to the NIST Post-Quantum Cryptography Standardization Project [NIS], 2020. <https://pq-crystals.org/dilithium/>.
- [ABD⁺20b] Roberto Avanzi, Joppe Bos, Léo Ducas, Eike Kiltz, Tancrede Lepoint, Vadim Lyubashevsky, John M. Schanck, Peter Schwabe, Gregor Seiler, and Damien Stehlé. CRYSTALS–Kyber. Submission to the NIST Post-Quantum Cryptography Standardization Project [NIS], 2020. <https://pq-crystals.org/kyber/>.
- [ACC⁺21] Erdem Alkim, Dean Yun-Li Cheng, Chi-Ming Marvin Chung, Hülya Evkan, Leo Wei-Lun Huang, Vincent Hwang, Ching-Lin Trista Li, Ruben Niederhagen, Cheng-Jhih Shih, Julian Wälde, and Bo-Yin Yang. Polynomial multiplication in NTRU prime comparison of optimization strategies on Cortex-M4. *IACR Trans. Cryptogr. Hardw. Embed. Syst.*, 2021(1):217–238, 2021. <https://doi.org/10.46586/tches.v2021.i1.217-238>.
- [ARM] ARM. Cortex-a72 software optimization guide. <https://developer.arm.com/documentation/uan0016/a/>.
- [Bar86] Paul Barrett. Implementing the Rivest Shamir and Adleman public key encryption algorithm on a standard digital signal processor. In *CRYPTO 1986*, LNCS, pages 311–323. Springer, 1986.
- [BKS19] Leon Botros, Matthias J. Kannwischer, and Peter Schwabe. Memory-efficient high-speed implementation of Kyber on Cortex-M4. In *Progress in Cryptology - AFRICACRYPT 2019*, volume 11627 of *Lecture Notes in Computer Science*, pages 209–228. Springer, 2019. https://doi.org/10.1007/978-3-030-23696-0_11.
- [CHK⁺21] Chi-Ming Marvin Chung, Vincent Hwang, Matthias J. Kannwischer, Gregor Seiler, Cheng-Jhih Shih, and Bo-Yin Yang. NTT multiplication for NTT-unfriendly rings new speed records for Saber and NTRU on Cortex-M4 and AVX2. *IACR Trans. Cryptogr. Hardw. Embed. Syst.*, 2021(2):159–188, 2021. <https://doi.org/10.46586/tches.v2021.i2.159-188>.
- [DKRV20] Jan-Pieter D’Anvers, Angshuman Karmakar, Sujoy Sinha Roy, and Frederik Vercauteren. SABER. Submission to the NIST Post-Quantum Cryptography Standardization Project [NIS], 2020. <https://www.esat.kuleuven.be/cosic/pqcrypto/saber/>.
- [GKS21] Denisa O. C. Greconici, Matthias J. Kannwischer, and Daan Sprenkels. Compact dilithium implementations on Cortex-M3 and Cortex-M4. *IACR Trans. Cryptogr. Hardw. Embed. Syst.*, 2021(1):1–24, 2021. <https://doi.org/10.46586/tches.v2021.i1.1-24>.

- [Har14] David Harvey. Faster arithmetic for number-theoretic transforms. *Journal of Symbolic Computation*, 60:113–119, 2014.
- [HHK17] Dennis Hofheinz, Kathrin Hövelmanns, and Eike Kiltz. A modular analysis of the Fujisaki-Okamoto transformation. In *Theory of Cryptography*, volume 10677, pages 341–371, 2017. <https://eprint.iacr.org/2017/604>.
- [LS19] Vadim Lyubashevsky and Gregor Seiler. NTTRU: truly fast NTRU using NTT. *IACR Trans. Cryptogr. Hardw. Embed. Syst.*, 2019(3):180–201, 2019. <https://doi.org/10.13154/tches.v2019.i3.180-201>.
- [Mon85] Peter L. Montgomery. Modular multiplication without trial division. *Mathematics of Computation*, 44:519–521, 1985. <https://www.ams.org/journals/mcom/1985-44-170/S0025-5718-1985-0777282-X>.
- [NG21] Duc Tri Nguyen and Kris Gaj. Optimized software implementations of CRYSTALS-Kyber, NTRU, and Saber using NEON-based special instructions of ARMv8. <https://csrc.nist.gov/CSRC/media/Events/third-pqc-standardization-conference/documents/accepted-papers/nguyen-optimized-software-gmu-pqc2021.pdf>, 2021. Third PQC Standardization Conference.
- [NIS] NIST, the US National Institute of Standards and Technology. Post-quantum cryptography standardization project. <https://csrc.nist.gov/Projects/post-quantum-cryptography>.
- [Sei18] Gregor Seiler. Faster AVX2 optimized NTT multiplication for Ring-LWE lattice cryptography. Cryptology ePrint Archive, Report 2018/039, 2018. <https://eprint.iacr.org/2018/039>.
- [Sho97] Peter W. Shor. Polynomial-time algorithms for prime factorization and discrete logarithms on a quantum computer. *SIAM Journal on Computing*, 26(5):1484–1509, October 1997.
- [SKS⁺21] Pakize Sanal, Emrah Karagoz, Hwajeong Seo, Reza Azarderakhsh, and Mehran Mozaffari Kermani. Kyber on ARM64: compact implementations of Kyber on 64-bit ARM Cortex-A processors. Cryptology ePrint Archive, Report 2021/561, 2021. <https://eprint.iacr.org/2021/561>.
- [TOP20] TOP500. Top500 November 2020, 2020. <https://www.top500.org/lists/top500/2020/11/>.
- [TOP21] TOP500. Top500 June 2021, 2021. <https://www.top500.org/lists/top500/2021/06/>.
- [Wes] Bas Westerbaan. Keccak-f1600 on aarch64. <https://github.com/bwesterb/armed-keccak>.

A Kyber CPA PKE

Algorithms 20–22 ([ABD⁺20b]), are the CPA-secure key generation, encryption, and decryption for the Kyber PKE.

Here the module is of dimension ℓ over the ring $R_q = \mathbb{Z}_q[x]/\langle x^n + 1 \rangle$, with $q = 3329$ and $n = 256$; Sample_U samples from the uniform distribution; Sample_B samples from a centered binomial (η fair coins); and Expand samples a seed into a uniform matrix of polynomials. Notice that A is sampled in (incomplete) NTT domain directly.

Algorithm 20 Kyber Key Generation

Output: $pk = (\text{seed}_A, \text{NTT}(b)), sk = (\text{NTT}(s))$

- 1: $\text{seed}_A \leftarrow \text{Sample}_U()$
 - 2: $\text{NTT}(A) \in R_q^{\ell \times \ell} \leftarrow \text{Expand}(\text{seed}_A)$
 - 3: $s, e \in R_q^\ell \leftarrow \text{Sample}_B()$
 - 4: $b \leftarrow A^T \cdot s + e$
-

Algorithm 22 Kyber CPA Decryption

Input: $ct = (c', b''), sk = (\text{NTT}(s))$

Output: m

- 1: $c \leftarrow \text{Decompress}(c', d_1)$
 - 2: $b' \leftarrow \text{Decompress}(b'', d_2)$.
 - 3: $m \leftarrow b' - c^T s$
-

Algorithm 21 Kyber CPA Encryption

Input: $m, r, pk = (\text{seed}_A, \text{NTT}(b))$

Output: $ct = (c', b'')$

- 1: $\text{NTT}(A) \in R_q^{\ell \times \ell} \leftarrow \text{Expand}(\text{seed}_A)$
 - 2: $s', e' \in R_q^\ell, e'' \in R_q \leftarrow \text{Sample}_B(r)$
 - 3: $c \leftarrow A s' + e'$
 - 4: $b' \leftarrow b^T s' + e'' + m$
 - 5: $ct \leftarrow \text{Compress}(c, d_1), \text{Compress}(b', d_2)$
-

$$\text{Compress}(x, d) = \lceil (2^d/q)x \rceil \bmod 2^d$$

$$\text{Decompress}(x, d) = \lceil (q/2^d)x \rceil$$

B Saber CPA PKE

Algorithms 23–25 ([DKRV20]), are CPA-secure key generation, encryption, and decryption for the Saber PKE. Here, the module is of dimension ℓ over the $R_q = \mathbb{Z}_q[x]/\langle x^n + 1 \rangle$, with $q = 2^{13}$ and $n = 256$; Sample_U samples from the uniform distribution; Sample_B samples from a centered binomial (η fair coins); and Expand samples a seed into a uniform matrix of polynomials.

Algorithm 23 Saber Key Generation

Output: $pk = (\text{seed}_A, b), sk = (s)$

- 1: $\text{seed}_A \leftarrow \text{Sample}_U()$
 - 2: $A \in R_q^{\ell \times \ell} \leftarrow \text{Expand}(\text{seed}_A)$
 - 3: $s \in R_q^\ell \leftarrow \text{Sample}_B()$
 - 4: $b \leftarrow \text{Round}(A^T \cdot s)$
-

Algorithm 25 Saber CPA Decryption

Input: $ct = (c, b'), sk = (s)$

Output: m

- 1: $v \leftarrow b'^T (s \bmod p)$
 - 2: $m \leftarrow \text{Round}(v - 2^{\epsilon_p - \epsilon_T} c \bmod p)$
-

Algorithm 24 Saber CPA Encryption

Input: $m, r, pk = (\text{seed}_A, b)$

Output: $ct = (c, b')$

- 1: $A \in R_q^{\ell \times \ell} \leftarrow \text{Expand}(\text{seed}_A)$
 - 2: $s' \in R_q^\ell \leftarrow \text{Sample}_B(r)$
 - 3: $b' \leftarrow \text{Round}(A s')$
 - 4: $v' \leftarrow b^T (s' \bmod p)$
 - 5: $c \leftarrow \text{Round}(v' - 2^{\epsilon - 1} m)$
-

Round is to nearest multiple of T .

C Dilithium

Algorithm 26, Algorithm 27, and Algorithm 28 show the Dilithium key generation, signature generation, and verification (resp.). S_η is the uniform distribution $\{-\eta, -\eta + 1, \dots, +\eta\}$; \parallel denotes concatenation; and $\|\cdot\|_\infty$ the sup-norm. For seed expansion functions ExpandA and

ExpandMask are used; for details about the rounding functions Power2Round, HighBits, and Decompose and the hint functions MakeHint and UseHint please see [ABD⁺20a].

Algorithm 26 Dilithium key generation

Output: $sk = (r, K, tr, s_1, s_2, t_0)$
Output: $pk = (r, t_1)$

- 1: $r \leftarrow \{0, 1\}^{256}$
- 2: $K \leftarrow \{0, 1\}^{256}$
- 3: $(s_1, s_2) \leftarrow S_\eta^\ell \times S_\eta^k$
- 4: $\text{NTT}(A) \in R_q^{k \times \ell} \leftarrow \text{ExpandA}(r)$
- 5: $t \leftarrow As_1 + s_2$
- 6: $(t_1, t_0) \leftarrow \text{Power2Round}(t)$
- 7: $tr \in \{0, 1\}^{256} \leftarrow \mathcal{H}(r || t_1)$

Algorithm 27 Dilithium signature generation

Input: $sk = (r, K, tr, s_1, s_2, t_0)$
Input: Message $M \in \{0, 1\}^*$
Output: Signature $\sigma = (z, h, \tilde{c})$

- 1: $\text{NTT}(A) \in R_q^{k \times \ell} := \text{ExpandA}(r)$
- 2: $\mu \in \{0, 1\}^{512} \leftarrow \mathcal{H}(tr || M)$
- 3: $\kappa \leftarrow 0; (z, h) \leftarrow \perp$
- 4: $r' \in \{0, 1\}^{512} \leftarrow \mathcal{H}(K || \mu)$
- 5: **while** $(z, h) = \perp$ **do**
- 6: $y \in S_{\gamma_1 - 1}^\ell \leftarrow \text{ExpandMask}(r', \kappa)$
- 7: $w \leftarrow Ay; w_1 \leftarrow \text{HighBits}(w)$
- 8: $\tilde{c} \in \{0, 1\}^{256} \leftarrow \mathcal{H}(\mu || w_1)$
- 9: $\text{NTT}(c) \leftarrow \text{NTT}(\mathcal{H}_B(\tilde{c}))$
- 10: $z \leftarrow y + cs_1$
- 11: $r_0 \leftarrow \text{LowBits}(w - cs_2)$
- 12: **if** $\|z\|_\infty \geq \gamma_1 - \beta$ **or** $\|r_0\|_\infty \geq \gamma_2 - \beta$ **then**
- 13: $(z, h) = \perp$
- 14: **else**
- 15: $h \leftarrow \text{MakeHint}(-ct_0, w - cs_2 + ct_0)$
- 16: **if** $\|ct_0\|_\infty \geq \gamma_2$ **or** $\# \text{ 1's in } h > \omega$ **then**
- 17: $(z, h) = \perp$
- 18: **end if**
- 19: **end if**
- 20: $\kappa \leftarrow \kappa + 1$
- 21: **end while**

Algorithm 28 Dilithium verification

Input: $pk = (r, \mathbf{t}_1)$
Input: Message $M \in \{0, 1\}^*$
Input: Signature $\sigma = (\mathbf{z}, \mathbf{h}, \tilde{c})$
Output: Valid or Invalid

- 1: $\text{NTT}(A) \in R_q^{k \times \ell} \leftarrow \text{ExpandA}(r)$
- 2: $\mu \in \{0, 1\}^{384} \leftarrow \mathcal{H}(\mathcal{H}(r || \mathbf{t}_1) || M)$
- 3: $c \leftarrow \mathcal{H}_B(\tilde{c})$
- 4: $w'_1 \leftarrow \text{UseHint}(h, Az - 2^d c t_1)$
- 5: **if** $\tilde{c} = \mathcal{H}(\mu || w'_1)$ **and** $\|z\|_\infty < \gamma_1 - \beta$ **and** $\# \text{ 1's in } h \leq \omega$ **then**
- 6: **return** Valid
- 7: **else**
- 8: **return** Invalid
- 9: **end if**

D Permutation in Dilithium and Kyber

Algorithm 29 Permutation of bottom 4 layers in Dilithium NTT.

Inputs:

$$\begin{aligned} \mathbf{a0} &= a_3 || a_2 || a_1 || a_0 \\ \mathbf{a1} &= a_7 || a_6 || a_5 || a_4 \\ \mathbf{a2} &= a_{11} || a_{10} || a_9 || a_8 \\ \mathbf{a3} &= a_{15} || a_{14} || a_{13} || a_{12} \end{aligned}$$

Outputs:

$$\begin{aligned} \mathbf{a0} &= a_{12} || a_8 || a_4 || a_0 \\ \mathbf{a1} &= a_{13} || a_9 || a_5 || a_1 \\ \mathbf{a2} &= a_{14} || a_{10} || a_6 || a_2 \\ \mathbf{a3} &= a_{15} || a_{11} || a_7 || a_3 \end{aligned}$$

- 1: trn1 t0.4S, a0.4S, a1.4S
 - 2: trn2 t1.4S, a0.4S, a1.4S
 - 3: trn1 t2.4S, a2.4S, a3.4S
 - 4: trn2 t3.4S, a2.4S, a3.4S
 - 5: trn1 a0.2D, t0.2D, t2.2D
 - 6: trn2 a2.2D, t0.2D, t2.2D
 - 7: trn1 a1.2D, t1.2D, t3.2D
 - 8: trn2 a3.2D, t1.2D, t3.2D
-

Algorithm 30 Permutation of bottom 3 layers of Kyber NTT.

Inputs:

$$\begin{aligned} *src0 &= (a0a1, a2a3, \dots, a30a31) \\ *src1 &= (a64a65, a66a67, \dots, a94a95) \end{aligned}$$

Outputs:

$$\begin{aligned} v24 &= (a0a1, a64a65, a16a17, a80a81) \\ v25 &= (a2a3, a66a67, a18a19, a82a83) \\ v26 &= (a4a5, a68a69, a20a21, a84a85) \\ v27 &= (a6a7, a70a71, a22a23, a86a87) \\ v28 &= (a8a9, a72a73, a24a25, a88a89) \\ v29 &= (a10a11, a74a75, a26a27, a90a91) \\ v30 &= (a12a13, a76a77, a28a29, a92a93) \\ v31 &= (a14a15, a78a79, a30a31, a94a95) \end{aligned}$$

- 1: ld4 {v16.4S, v17.4S, v18.4S, v19.4S}, [src0]
- 2: ld4 {v20.4S, v21.4S, v22.4S, v23.4S}, [src1]
- 3: trn1 v24.4S, v16.4S, v20.4S
- 4: trn2 v28.4S, v16.4S, v20.4S
- 5: trn1 v25.4S, v17.4S, v21.4S
- 6: trn2 v29.4S, v17.4S, v21.4S
- 7: trn1 v26.4S, v18.4S, v22.4S
- 8: trn2 v30.4S, v18.4S, v22.4S
- 9: trn1 v27.4S, v19.4S, v23.4S
- 10: trn2 v31.4S, v19.4S, v23.4S

E Assembly for Asymmetric Multiplication

Algorithm 31 `_4x4_asymmetric` as a building block for 32-bit 4×4 asymmetric multiplication in `saber`.

Inputs:

`mulacc, mulacc2, a0, b0, ..., b3, l0, h0, ..., l3, h3, dS, qS, dD`

Roles of the symbols:

Long multiplication with optional accumulations: `mulacc, mulacc2`

Coefficient of the NTT of matrix: `a0`

Coefficients of the NTT_heavy of vector: `b0, ..., b3`

Accumulators for double-size results: `l0, h0, ..., l3, h3`

Specifiers: `dS, qS, dD = (.2S, .4S, .2D)`

Outputs:

Case `(mulacc, mulacc2) = (smul1, smul2)`:

`l0 + h0 < 32 = a0 * b0, ..., l3 + h3 < 32 = a0 * b3`

Case `(mulacc, mulacc2) = (smla1, smla2)`:

`l0 + h0 < 32 += a0 * b0, ..., l3 + h3 < 32 += a0 * b3`

- 1: `mulacc l0dD, a0dS, b0dS`
 - 2: `mulacc2 h0dD, a0qS, b0qS`
 - 3: `mulacc l1dD, a0dS, b1dS`
 - 4: `mulacc2 h1dD, a0qS, b1qS`
 - 5: `mulacc l2dD, a0dS, b2dS`
 - 6: `mulacc2 h2dD, a0qS, b2qS`
 - 7: `mulacc l3dD, a0dS, b3dS`
 - 8: `mulacc2 h3dD, a0qS, b3qS`
-

Algorithm 32 qq_montgomery for 16 parallel 32-bit Montgomery reductions.

Inputs:

$c_0, \dots, c_3, l_0, \dots, l_3, h_0, \dots, h_3, t_0, \dots, t_3, Q_{\text{prime}}, Q, d_S, q_S, d_D$

Roles of the symbols:

Output registers: c_0, \dots, c_3

64-bit value to be reduced: $l_0 + h_0 \ll 32, \dots, l_3 + h_3 \ll 32$

Auxiliary registers: t_0, \dots, t_3

Specifiers: $(d_S, q_S, d_D) = (.2S, .4S, .2D)$

Outputs:

$c_0 = (l_0 + h_0 \ll 32)32^{-1} \bmod Q, \dots, c_3 = (l_3 + h_3 \ll 32)32^{-1} \bmod Q$

```

1: uzp1 t0qS, l0qS, h0qS
2: uzp1 t1qS, l1qS, h1qS
3: uzp1 t2qS, l2qS, h2qS
4: uzp1 t3qS, l3qS, h3qS
5: mul t0qS, t0qS, QprimeqS
6: mul t1qS, t1qS, QprimeqS
7: mul t2qS, t2qS, QprimeqS
8: mul t3qS, t3qS, QprimeqS
9: smlal l0dD, t0dS, QdS
10: smlal2 h0dD, t0qS, QqS
11: smlal l1dD, t1dS, QdS
12: smlal2 h1dD, t1qS, QqS
13: smlal l2dD, t2dS, QdS
14: smlal2 h2dD, t2qS, QqS
15: smlal l3dD, t3dS, QdS
16: smlal2 h3dD, t3qS, QqS
17: uzp2 c0qS, l0qS, h0qS
18: uzp2 c1qS, l1qS, h1qS
19: uzp2 c2qS, l2qS, h2qS
20: uzp2 c3qS, l3qS, h3qS

```

Algorithm 33 4 parallel 32-bit better accumulations for asymmetric multiplications (for saber).

Inputs:

Source registers: x0 for a_0 , x1 for b_0 , x2 for $b'_0 = \omega b_0$, x4 for a_1 , x5 for b_1 , x6 for $b'_1 = \omega b_1$, x8 for a_2 , x9 for b_2 , x10 for $b'_2 = \omega b_2$

Accumulators: v16, v20, v17, v21, v18, v22, v19, v23

Output registers: v24, v25, v26, v27

Symbols:

mul_long = smull, smull2

m1a_long = smlal, smlal2

acc_long = v16, v20, v17, v21, v18, v22, v19, v23

acc_long_T = v16, v17, v18, v19, v20, v21, v22, v23

T0 = v0, v1, v2, v3

T1 = v4, v5, v6, v7

T2 = v8, v9, v10, v11

T3 = v12, v13, v14, v15

C = v24, v25, v26, v27

Outputs:

$v24 + v25x + v26x^2 + v27x^3 = (a_0 * b_0 + a_1 * b_1 + a_2 * b_2)32^{-1} \bmod (x^4 - \omega)$

```

1: ld4 { T0}, [ x0]
2: ld4 { T1}, [ x1]
3: ld4 { T2}, [ x2]
4: _4x4_asymmetric mul_long, v3, v9, v10, v11, v4, acc_long
5: _4x4_asymmetric m1a_long, v2, v10, v11, v4, v5, acc_long
6: _4x4_asymmetric m1a_long, v1, v11, v4, v5, v6, acc_long
7: _4x4_asymmetric m1a_long, v0, v4, v5, v6, v7, acc_long
8: ld4 { T3}, [ x4]
9: ld4 { C}, [ x5]
10: ld4 { T2}, [ x6]
11: _4x4_asymmetric m1a_long, v15, v9, v10, v11, v24, acc_long
12: _4x4_asymmetric m1a_long, v14, v10, v11, v24, v25, acc_long
13: _4x4_asymmetric m1a_long, v13, v11, v24, v25, v26, acc_long
14: _4x4_asymmetric m1a_long, v12, v24, v25, v26, v27, acc_long
15: ld4 { T0}, [ x8]
16: ld4 { T1}, [ x9]
17: ld4 { T2}, [x10]
18: _4x4_asymmetric m1a_long, v3, v9, v10, v11, v4, acc_long
19: _4x4_asymmetric m1a_long, v2, v10, v11, v4, v5, acc_long
20: _4x4_asymmetric m1a_long, v1, v11, v4, v5, v6, acc_long
21: _4x4_asymmetric m1a_long, v0, v4, v5, v6, v7, acc_long
22: qq_montgomery C, acc_long_T, v0, v1, v2, v3, Qprime, Q
23: st4 { C}, [x11]

```

F Assembly for Interleaved Multi-Layer Butterflies

Algorithm 34 qq_butterfly_top for 16 parallel 32-bit Montgomery multiplications.

Inputs:

$a_0, \dots, a_3, b_0, \dots, b_3, t_0, \dots, t_3, \text{mod}, z_0, l_0, h_0, \dots, z_3, l_3, h_3, q_S, s_S$

Roles of the symbols:

Operating registers: $a_0, \dots, a_3, b_0, \dots, b_3, t_0, \dots, t_3$

Registers with twiddle factors: z_0, \dots, z_3

Indices for twiddle factors: $l_0, \dots, l_3, h_0, \dots, h_3$

Modulus: mod

Specifiers: $(q_S, s_S) = (.4S, .S)$

Outputs:

$t_0 = b_0 \omega_0 \bmod^{\pm} q, \dots, t_3 = b_3 \omega_3 \bmod^{\pm} q$

```

1: mul t0qS, b0qS, z0sS[h0]
2: mul t1qS, b1qS, z1sS[h1]
3: mul t2qS, b2qS, z2sS[h2]
4: mul t3qS, b3qS, z3sS[h3]
5: sqrdmulh b0qS, b0qS, z0sS[l0]
6: sqrdmulh b1qS, b1qS, z1sS[l1]
7: sqrdmulh b2qS, b2qS, z2sS[l2]
8: sqrdmulh b3qS, b3qS, z3sS[l3]
9: mls t0qS, b0qS, modsS[0]
10: mls t1qS, b1qS, modsS[0]
11: mls t2qS, b2qS, modsS[0]
12: mls t3qS, b3qS, modsS[0]

```

Algorithm 35 qq_butterfly_bot for 16 parallel 32-bit sub-add pairs.

Inputs:

$a_0, \dots, a_3, b_0, \dots, b_3, t_0, \dots, t_3, \text{mod}, z_0, l_0, h_0, \dots, z_3, l_3, h_3, q_S, s_S$

Roles of the symbols:

Operating registers: $a_0, \dots, a_3, b_0, \dots, b_3, t_0, \dots, t_3$

Registers with twiddle factors: z_0, \dots, z_3

Indices for twiddle factors: $l_0, \dots, l_3, h_0, \dots, h_3$

Modulus: mod

Specifiers: $(q_S, s_S) = (.4_S, .S)$

Outputs:

$(a_0, b_0) = (a_0 + t_0, a_0 - t_0), \dots, (a_3, b_3) = (a_3 + t_3, a_3 - t_3)$

1: sub $b_{0q_S}, a_{0q_S}, t_{0q_S}$

2: sub $b_{1q_S}, a_{1q_S}, t_{1q_S}$

3: sub $b_{2q_S}, a_{2q_S}, t_{2q_S}$

4: sub $b_{3q_S}, a_{3q_S}, t_{3q_S}$

5: add $a_{0q_S}, a_{0q_S}, t_{0q_S}$

6: add $a_{1q_S}, a_{1q_S}, t_{1q_S}$

7: add $a_{2q_S}, a_{2q_S}, t_{2q_S}$

8: add $a_{3q_S}, a_{3q_S}, t_{3q_S}$

Algorithm 36 `qq_butterfly_mixed` for interleaving 16 parallel 32-bit CT butterflies.

Inputs:

$a_0, \dots, a_3, b_0, \dots, b_3, t_0, \dots, t_3, a_4, \dots, a_7, b_4, \dots, b_7, t_4, \dots, t_7, \text{mod}, z_0, 10, h_0, \dots, z_7, 17, h_7, qS, sS$

Roles of the symbols:

Operating registers set 1: $a_0, \dots, a_3, b_0, \dots, b_3, t_0, \dots, t_3$

Operating registers set 2: $a_4, \dots, a_7, b_4, \dots, b_7, t_4, \dots, t_7$

Registers with twiddle factors set 1: z_0, \dots, z_3

Registers with twiddle factors set 2: z_4, \dots, z_7

Indices for twiddle factors set 1: $10, \dots, 13, h_0, \dots, h_3$

Indices for twiddle factors set 2: $14, \dots, 17, h_4, \dots, h_7$

Modulus: `mod`

Specifiers: $(qS, sS) = (.4S, .S)$

Outputs:

$(a_0, b_0) = (a_0 + t_0, a_0 - t_0), \dots, (a_3, b_3) = (a_3 + t_3, a_3 - t_3),$

$t_4 = b_4 \omega_4 \bmod^{\pm} q, \dots, t_7 = b_7 \omega_7 \bmod^{\pm} q$

```

1: sub b0qS, a0qS, t0qS
2: mul t4qS, b4qS, z4sS[h4]
3: sub b1qS, a1qS, t1qS
4: mul t5qS, b5qS, z5sS[h5]
5: sub b2qS, a2qS, t2qS
6: mul t6qS, b6qS, z6sS[h6]
7: sub b3qS, a3qS, t3qS
8: mul t7qS, b7qS, z7sS[h7]
9: add a0qS, a0qS, t0qS
10: sqrdmulh b4qS, b4qS, z4sS[14]
11: add a1qS, a1qS, t1qS
12: sqrdmulh b5qS, b5qS, z5sS[15]
13: add a2qS, a2qS, t2qS
14: sqrdmulh b6qS, b6qS, z6sS[16]
15: add a3qS, a3qS, t3qS
16: sqrdmulh b7qS, b7qS, z7sS[17]
17: mls t4qS, b4qS, modsS[0]
18: mls t5qS, b5qS, modsS[0]
19: mls t6qS, b6qS, modsS[0]
20: mls t7qS, b7qS, modsS[0]

```

Algorithm 37 `qq_butterfly_mixed_rev` for interleaving 16 parallel 32-bit GS butterflies.

Inputs:

$a_0, \dots, a_3, b_0, \dots, b_3, t_0, \dots, t_3, a_4, \dots, a_7, b_4, \dots, b_7, t_4, \dots, t_7, \text{mod}, z_0, 10, h_0, \dots, z_7, 17, h_7, qS, sS$

Roles of the symbols:

Operating registers set 1: $a_0, \dots, a_3, b_0, \dots, b_3, t_0, \dots, t_3$

Operating registers set 2: $a_4, \dots, a_7, b_4, \dots, b_7, t_4, \dots, t_7$

Registers with twiddle factors set 1: z_0, \dots, z_3

Registers with twiddle factors set 2: z_4, \dots, z_7

Indices for twiddle factors set 1: $10, \dots, 13, h_0, \dots, h_3$

Indices for twiddle factors set 2: $14, \dots, 17, h_4, \dots, h_7$

Modulus: mod

Specifiers: $(qS, sS) = (.4S, .S)$

Outputs:

$(a_4, b_4) = (a_4 + t_4, a_4 - t_4), \dots, (a_7, b_7) = (a_7 + t_7, a_7 - t_7),$

$t_0 = b_0 \omega_0 \bmod^{\pm} q, \dots, t_3 = b_3 \omega_3 \bmod^{\pm} q$

- 1: `mul t0qS, b0qS, z0sS[h0]`
 - 2: `sub b4qS, a4qS, t4qS`
 - 3: `mul t1qS, b1qS, z1sS[h1]`
 - 4: `sub b5qS, a5qS, t5qS`
 - 5: `mul t2qS, b2qS, z2sS[h2]`
 - 6: `sub b6qS, a6qS, t6qS`
 - 7: `mul t3qS, b3qS, z3sS[h3]`
 - 8: `sub b7qS, a7qS, t7qS`
 - 9: `sqrddmulh b0qS, b0qS, z0sS[10]`
 - 10: `add a4qS, a4qS, t4qS`
 - 11: `sqrddmulh b1qS, b1qS, z1sS[11]`
 - 12: `add a5qS, a5qS, t5qS`
 - 13: `sqrddmulh b2qS, b2qS, z2sS[12]`
 - 14: `add a6qS, a6qS, t6qS`
 - 15: `sqrddmulh b3qS, b3qS, z3sS[13]`
 - 16: `add a7qS, a7qS, t7qS`
 - 17: `mls t0qS, b0qS, modsS[0]`
 - 18: `mls t1qS, b1qS, modsS[0]`
 - 19: `mls t2qS, b2qS, modsS[0]`
 - 20: `mls t3qS, b3qS, modsS[0]`
-

Algorithm 38 4 layers of 32-bit CT butterflies over 32 SIMD registers.

Inputs:Coefficients: $(v_0, \dots, v_{15}) = (a_0, \dots, a_{15})$ Auxiliary registers: $v_{16}, \dots, v_{19}, v_{28}, \dots, v_{31}$

Twiddle factors:

$$\begin{aligned} v_{20} &= h_0 || 10 || 0 || Q \\ v_{21} &= h_2 || 12 || h_1 || 11 \\ v_{22} &= h_4 || 14 || h_3 || 13 \\ v_{23} &= h_6 || 16 || h_5 || 15 \\ v_{24} &= h_8 || 18 || h_7 || 17 \\ v_{25} &= h_{10} || 110 || h_9 || 19 \\ v_{26} &= h_{12} || 112 || h_{11} || 111 \\ v_{27} &= h_{14} || 114 || h_{13} || 113 \end{aligned}$$

Symbols:L0_0 = $v_0, v_2, v_4, v_6, v_8, v_{10}, v_{12}, v_{14}$ L0_1 = $v_1, v_3, v_5, v_7, v_9, v_{11}, v_{13}, v_{15}$ L1_0 = $v_0, v_2, v_8, v_{10}, v_4, v_6, v_{12}, v_{14}$ L1_1 = $v_1, v_3, v_9, v_{11}, v_5, v_7, v_{13}, v_{15}$ L2_0 = $v_0, v_4, v_8, v_{12}, v_2, v_6, v_{10}, v_{14}$ L2_1 = $v_1, v_5, v_9, v_{13}, v_3, v_7, v_{11}, v_{15}$ L3_0 = $v_0, v_2, v_4, v_6, v_1, v_3, v_5, v_7$ L3_1 = $v_8, v_{10}, v_{12}, v_{14}, v_9, v_{11}, v_{13}, v_{15}$ T0 = $v_{16}, v_{17}, v_{18}, v_{19}$ T1 = $v_{28}, v_{29}, v_{30}, v_{31}$ mod = v_{20} W0 = $v_{20}, 2, 3, v_{20}, 2, 3, v_{20}, 2, 3, v_{20}, 2, 3$ W1 = $v_{21}, 0, 1, v_{21}, 0, 1, v_{21}, 2, 3, v_{21}, 2, 3$ W2 = $v_{22}, 0, 1, v_{22}, 2, 3, v_{23}, 0, 1, v_{23}, 2, 3$ W3_0 = $v_{24}, 0, 1, v_{24}, 2, 3, v_{25}, 0, 1, v_{25}, 2, 3$ W3_1 = $v_{26}, 0, 1, v_{26}, 2, 3, v_{27}, 0, 1, v_{27}, 2, 3$ **Outputs:** $(v_0, \dots, v_{15}) = \text{NTT}(a_0, \dots, a_{15})$

- 1: qq_butterfly_top L0_1, T0, mod, W0
 - 2: qq_butterfly_bot L0_1, T0, mod, W0
 - 3: qq_butterfly_top L0_0, T1, mod, W0
 - 4: qq_butterfly_bot L0_0, T1, mod, W0
 - 5: qq_butterfly_top L1_1, T0, mod, W1
 - 6: qq_butterfly_bot L1_1, T0, mod, W1
 - 7: qq_butterfly_top L1_0, T1, mod, W1
 - 8: qq_butterfly_bot L1_0, T1, mod, W1
 - 9: qq_butterfly_top L2_1, T0, mod, W2
 - 10: qq_butterfly_bot L2_1, T0, mod, W2
 - 11: qq_butterfly_top L2_0, T1, mod, W2
 - 12: qq_butterfly_bot L2_0, T1, mod, W2
 - 13: qq_butterfly_top L3_0, T0, mod, W3_0
 - 14: qq_butterfly_bot L3_0, T0, mod, W3_0
 - 15: qq_butterfly_top L3_1, T1, mod, W3_1
 - 16: qq_butterfly_bot L3_1, T1, mod, W3_1
-